sustainable chemistry

MDPI

Review

Cleaner Chemistry for Clean Energy: PFAS-Free Materials in PEM Electrochemical Technologies

Erasmo Salvatore Napolitano [1,*], Andrea Rosati [2], Alessia Bezzon [1], Ivan Moretti [3], Ana Suárez-Vega [4], Fabiola Brusciotti [4] and Angelo Meduri [1]

[1] RINA Consulting—Centro Sviluppo Materiali SpA, Zona Industriale San Pietro Lametino, Comparto 1, 88046 Lamezia Terme, Italy; alessia.bezzon@rina.org (A.B.); angelo.meduri@rina.org (A.M.)
[2] RINA Consulting—Centro Sviluppo Materiali SpA, Via di Castel Romano 100, 00128 Rome, Italy; andrea.rosati@rina.org
[3] Il Sentiero International Campus Srl, Via Friuli 11, 36015 Schio, Italy; ivan.moretti@ecor-international.com
[4] Tecnalia, Basque Research and Technology Alliance (BRTA), Mikeletegi Pasealekua 2, 20009 Donostia-San Sebastian, Spain; ana.suarez@tecnalia.com (A.S.-V.); fabiola.brusciotti@tecnalia.com (F.B.)
* Correspondence: erasmo.napolitano@rina.org

Abstract

Per- and polyfluoroalkyl substances (PFAS) have found wide application in proton exchange membrane fuel cells (PEMFCs) and water electrolysers (PEMELs), thanks to their exceptional chemical and thermal stability. However, their environmental persistence and growing regulatory pressure—particularly from the European Union—have made the transition to PFAS-free components a priority. This work reviews current advancements in alternative materials that can guarantee the same performance or maybe improve it. Although several non-fluorinated materials have demonstrated initial performance close to PFAS-based benchmarks, significant challenges remain. These include limited long-term stability, difficulties for new materials to fit into existing stack architectures, and the lack of standardized testing protocols. Nevertheless, recent efforts have successfully demonstrated a PFAS-free PEM electrolyser stack at TRL 4, validating the technical feasibility of full PFAS substitution. Achieving commercial readiness will require parallel progress in materials development and industrial scalability. This review highlights the possibility that hydrogen technologies, such as fuel cells and electrolysers, which are called upon to support the energy transition towards a more sustainable future, are themselves truly environmentally friendly, thus making their use as green as possible.

Keywords: PFAS-free membranes; proton exchange membrane fuel cells (PEMFC); PEM water electrolysers (PEMEL); sustainable materials

Check for updates

Academic Editor: Lathe Jones

Received: 5 March 2026
Revised: 9 April 2026
Accepted: 16 April 2026
Published: 23 April 2026

Copyright: © 2026 by the authors. Licensee MDPI, Basel, Switzerland. This article is an open access article distributed under the terms and conditions of the Creative Commons Attribution (CC BY) license.

1. Introduction

Per- and polyfluoroalkyl substances (PFAS) are a wide-ranging class of synthetic fluorinated chemicals distinguished by their multiple carbon–fluorine bonds—one of the strongest bonds in organic chemistry.

This molecular property gives excellent stability and resistance to heat and chemical attack to PFAS. They, moreover, possess unique surface properties: they can repel not only water, but also oil and dirt [1]. Thanks to these characteristics, PFAS have been used in various industrial and consumer applications [2]: they have a consolidated place in products of everyday life such as non-stick cookware (PTFE coatings), waterproof and stain-resistant textiles, food packaging, firefighting foams, and personal care products. On the

other hand, PFAS have crucial roles in high-performance sectors: for example, aerospace and automotive parts, semiconductor manufacturing, and various chemical processes all utilize PFAS-based polymers or surfactants. Glüge et al. [3] identified over 200 use categories spanning 64 industrial sectors for more than 1400 individual PFAS. It can be said that PFAS are materials present nearly everywhere in modern society, used for providing durability and functionalities that few other materials can reach [4]. However, the same properties that make PFAS so useful raise serious concerns about their environmental and health impacts: PFAS's extraordinary chemical stability means they cannot break down easily in the environment, earning them the nickname "forever chemicals".

Natural processes generally are not able to degrade the carbon–fluorine bonds, so PFAS released into soil, air, and water persist for decades or longer [5], resulting in their accumulation throughout ecosystems. Widespread monitoring has found PFAS residues almost everywhere, from groundwater [6] and crops [7] to wildlife and humans [8]. In fact, studies indicate that almost all people in industrialized nations have detectable PFAS traces in their blood serum: one U.S. CDC [9] survey in 2003–2004 reported PFAS in 98% of Americans tested.

Because most PFAS cannot really be metabolized or excreted, they bioaccumulate in food chains and in human tissues with repeated exposure [10]. PFAS are now recognized as toxic or potentially toxic: they can act as endocrine-disrupting chemicals, interfere with metabolic and immune functions, and some have been associated with developmental defects and cancers in epidemiological studies [11,12]. For example, elevated PFAS levels correlate with suppressed antibody responses to vaccines [13] and with lower birth weights in infants [14]. The liver and kidneys are key target organs for PFAS exposure, which has been linked to non-alcoholic fatty liver disease and reduced kidney function [15], among other effects [16].

Although research is ongoing to fully explain the mechanisms, the scientific community agrees that continued environmental buildup of PFAS represents an "unacceptable risk" [17], a diffuse pollution problem that could silently push exposed populations to pass over the health thresholds.

The awareness of PFAS effects has led regulators worldwide to pursue stringent limitations on their production and use. As an example of the most stringent, authorities in the European Union are advancing a proposal to restrict nearly all PFAS under the EU chemicals framework (REACH). In early 2023, environmental agencies from five countries (Germany, the Netherlands, Denmark, Sweden, and Norway) submitted a sweeping restriction dossier to the European Chemicals Agency (ECHA) covering an estimated 10,000–12,000 PFAS [18]. The proposal asked for a ban on PFAS in most applications, with only a few exemptions for very essential uses (i.e., critical to society and lacking alternatives) [19]. Regulators argue that treating PFAS as a class is necessary, given that all PFAS share the problematic trait of persistence, and reason that continued emissions will lead to ever-increasing contamination over time in the global environment. ECHA itself describes the PFAS plan as "the broadest restriction proposal under REACH so far". If adopted, the rule would force a phase-out of non-essential PFAS uses after designated transition periods [19]. However, the overall intent is clear: to shrink PFAS usage to a minimum across Europe in the coming decade.

Still, implementing a comprehensive ban faces practical challenges. PFAS are so deeply ingrained in modern technology that sweeping restrictions could disrupt industries ranging from electronics to green tech. Among the sectors raising urgent concern about the EU proposal are the clean energy industries—notably batteries, fuel cells, and electrolysers [20]—which today rely heavily on PFAS-based materials.

This has set up a tense debate between environmental regulators and industry proponents of so-called "necessary uses".

Clean energy technologies like water electrolysers (PEMELs) and proton exchange membrane fuel cells (PEMFCs) are widely indicated as solutions for decarbonizing transportation and energy [21]. These systems enable the hydrogen economy by efficiently converting hydrogen to electricity (fuel cell mode) or electricity to hydrogen (electrolyzer mode). However, it is an uncomfortable reality that today PEM fuel cells and electrolysers are fundamentally constructed from PFAS-containing components [22]. In fact, PFAS-based polymers are almost in every part of a typical PEM stack, owing to their unrivalled performance under the harsh, corrosive conditions inside these devices. This dependence creates a stark paradox. Technologies that are key to reducing environmental pollution (zero-emission vehicles and renewable energy storage) are themselves made with persistent pollutants. Industry experts openly acknowledge that no fully equivalent substitutes exist today for PFAS in certain fuel cell applications—fluoropolymers are uniquely capable of meeting the demanding requirements (high proton flux, thermal stability, chemical inertness) inside PEM devices [23]. Thus, the prospect of an abrupt PFAS ban has raised alarm in the hydrogen and fuel cell sector [24]. In 2023, the European industry group Hydrogen Europe warned that a blanket ban on PFAS could "severely inhibit" the rollout of hydrogen technologies, arguing that fluoropolymer-based membranes and components are currently essential and irreplaceable in many fuel cell and electrolyzer designs. Regulators, for their part, have signalled they do not intend to derail green technologies—any PFAS restrictions will likely include temporary exemptions for truly critical uses like medical inhalers and possibly fuel cells. Nevertheless, the writing is on the wall: in the long term, even energy technologies must become PFAS-free to align with the "toxic-free environment" goals of policies like the EU Chemicals Strategy for Sustainability [25]. The imperative is clear: enabling truly clean hydrogen and fuel cell systems will require purging PFAS from their design. This realization has set off an intense effort in labs and startups worldwide to invent PFAS-free alternatives, as discussed next. This growing attention is also reflected in the scientific literature. Figure 1 shows a pronounced increase in PFAS-related publications over the last two decades, with only limited activity in the early 2000s, followed by a gradual rise up to the mid-2010s and a sharp acceleration from 2018 onward. The particularly steep growth observed after 2020 indicates that PFAS have become a central topic in contemporary materials, environmental, and regulatory research. This expanding literature reflects the increasing scientific and industrial attention devoted to the persistence, toxicity, and substitution of fluorinated compounds. In this context, a critical and structured review focused on PFAS-free materials in PEM electrochemical technologies is timely, as it provides an organized framework to rationalize the rapidly growing body of studies, compare the emerging alternatives, and identify the main challenges that still limit practical implementation.

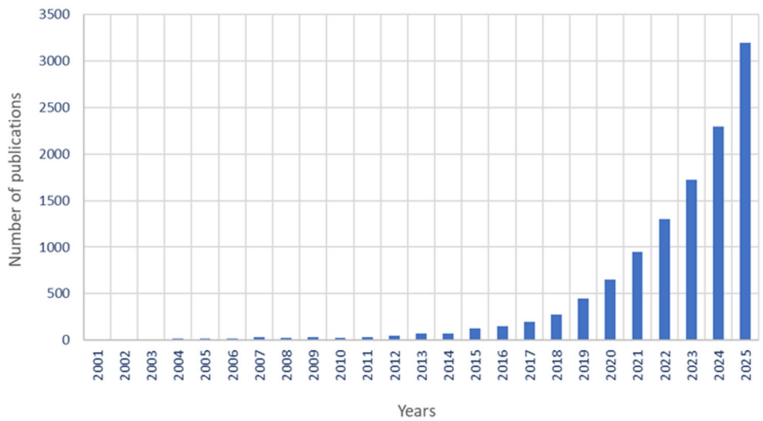


Figure 1. Annual number of PFAS-related publications (Scopus, query TITLE-ABS-KEY (PFAS OR ("Per- and polyfluoroalkyl substances"))).

2. PEM Device Architecture and the Quantitative Relevance of PFAS Use

Figure 2 shows an exploded view of a single-stack PEM fuel cell. In an actual PEM stack, many of these elementary units are assembled in series between end plates in order to achieve the desired voltage and power output. Each unit includes bipolar plates with flow fields, sealing gaskets, gas diffusion layers, and the membrane-based electrochemical core. In the following sections, the role of each component will be briefly examined, and current research efforts aimed at replacing PFAS with safer, fluorine-free alternatives will be explored.

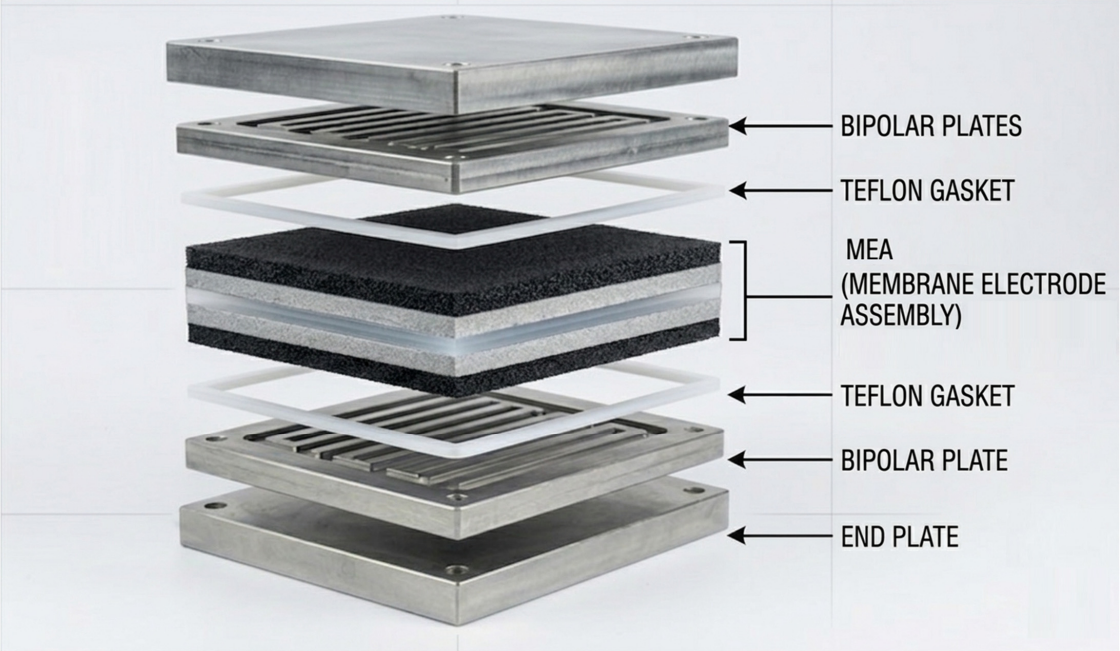


Figure 2. Schematic of a single-stack PEM fuel cell [26].

In PEM-based electrochemical devices, the membrane–electrode assembly (MEA), or more generally the membrane-based electrochemical core, is the functional core of the cell.

In PEM fuel cells, the MEA is also a major cost driver and has been reported to account for around 70% of the total PEMFC cost, highlighting its technological and economic importance [27]. In PEM fuel cells, the MEA is composed of the proton exchange membrane sandwiched between the anode and cathode catalyst layers, which are in turn coupled to gas diffusion layers and, frequently, to microporous layers for reactant distribution and water management. This multilayer assembly is then compressed between bipolar plates and seals to form the repeating unit of the stack [28,29]. A closely related architecture applies to PEM water electrolysers, where the cell is built around a membrane-based electrochemical core coupled with porous transport layers and bipolar plates containing flow channels [30]. In both technologies, the membrane is not simply a passive separator: it provides proton conduction, gas separation, and electrochemical coupling between the two electrodes, while ionomer-containing catalyst layers and transport layers ensure the simultaneous control of charge transport, reactant supply, and product removal [31,32]. As a result, PFAS dependence is embedded in the most performance-critical region of the device rather than being limited to secondary or auxiliary components.

Quantitative Relevance of PFAS Use in PEM Technologies

Although public PFAS inventories do not isolate PEM fuel cells and PEM water electrolysers as a standalone tonnage category, they are explicitly included within the broader energy sector in the updated European PFAS restriction dossier. For the EEA in

2020, this sector falls within the 1000–10,000 t year^{-1} PFAS use band, below the largest PFAS-consuming sectors but still clearly non-negligible [33]. The strategic relevance of PEM technologies becomes even clearer when the PFAS content is normalized to power output. Using the literature values for dry PFSA membrane density (~2.0 g cm^{-3}) and thicknesses reported for common benchmark membranes (183 µm for Nafion® 117 and 50 µm for Nafion® 212 (Chemours, Wilmington, DE, USA)) [34–36], a membrane-only estimate already yields a substantial fluoropolymer inventory. For PEM water electrolysis, representative operation at about 2 A cm^{-2} and roughly 1.8–2.0 V corresponds to an areal power density of approximately 3.6–4.0 W cm^{-2}, which translates to a membrane requirement on the order of 9–10 kg MW^{-1} [34,35]. For PEM fuel cells, the widely used benchmark of about 1.0 W cm^{-2} leads to a membrane inventory of about 10 kg MW^{-1} when combined with the literature thickness of Nafion® 212 and the same dry PFSA density [36,37]. These values are conservative lower-bound estimates because they refer only to the membrane and do not include PFSA ionomer in the catalyst layers or fluorinated hydrophobic agents in porous media. Their importance is amplified by market expansion: global installed water-electrolyser capacity reached 1.4 GW at the end of 2023, and announced projects suggest a potential scale-up toward 230–520 GW by 2030 [32]. Taken together, these data indicate that PEM technologies are not yet the dominant PFAS-use sector by mass, but they already combine a non-trivial fluoropolymer intensity per MW with a rapidly growing deployment trajectory, which makes them a highly relevant target for PFAS substitution [32,33].

3. PFAS-Dependent Components and Replacement Pathways in PEM Devices

Having established the functional role of PFAS-containing components within PEM devices and the growing strategic relevance of this application sector, the discussion can now move from problem definition to material replacement strategies. The transition toward PFAS-free PEM technologies does not rely on a single substitute, but rather on a component-specific redesign approach, since each element of the stack performs distinct electrochemical, transport, sealing, or structural functions. For this reason, the following sections examine the main PFAS-dependent components individually and discuss the most relevant PFAS-free alternatives, together with their current advantages, limitations, and technological maturity.

3.1. Proton-Conducting Membranes: PFAS Benchmarks and PFAS-Free Alternatives

A well-functioning PEM possesses several key characteristics. Primarily, it must selectively permit proton transport while effectively blocking the passage of electrons. Crucially, it also acts as a barrier, preventing the direct mixing of fuel and oxygen, which would compromise cell efficiency and safety. Given that most fuel cells operate under dynamic conditions, the PEM must exhibit robust stability, maintaining performance even in challenging or fluctuating environments. Furthermore, adequate water retention within the membrane is essential; this not only supports efficient proton flow but also minimizes internal resistance. However, it is important to note that excessive water uptake can lead to membrane swelling, which may negatively impact overall performance [38]. For the purposes of this review, proton-conducting membranes can first be distinguished according to their main operating temperature window, namely, low-temperature PEMs and intermediate-temperature PEMs. Low-temperature PEMs typically include PFSA-based and other hydrated proton-conducting membranes, whereas intermediate-temperature PEMs are generally represented by acid-doped polybenzimidazole systems. The polymeric membranes discussed in the literature can be arranged according to decreasing

fluorine content as follows: (1) perfluorinated membranes, such as perfluorosulfonic acid membranes; (2) perfluorinated composite membranes, such as PTFE/Nafion® composite systems; (3) partially fluorinated membranes, such as styrene-grafted and sulfonated poly(vinylidene fluoride); and (4) fluorine-free membranes, including both non-fluorinated composite membranes, such as acid-doped polybenzimidazoles, and non-fluorinated membranes based on the incorporation of sulfonic acid groups into aromatic polymers, such as sulfonated polybenzimidazole, polyimides, and polyphenylene [27,39].

3.1.1. Benchmark PFAS Membrane: Nafion® and Current Fluorinated Design Strategies

Among fluorinated proton-conducting membranes, Nafion® stands as the benchmark material for PEM applications. This PFAS material was first developed by DuPont in the 1960s [40]. Its discovery was an unforeseen outcome of optimizing a Teflon-based material. Nafion® is obtained by copolymerizing tetrafluoroethylene (TFE) with a sulfonyl fluoride—containing perfluoro(alkyl vinyl ether), extruding the polymer into films, converting—SO_2F to $-SO_3Na$ with hot NaOH, then protonating to sulfonic acid, $-SO_3H$ [41].

The effectiveness of Nafion® is mainly associated with the presence of $-SO_3H$. When hydrated, these groups hydrolyse to SO_3^- and H_3O^+, enabling efficient proton transport and significantly boosting the material's protonic conductivity. For this reason, Nafion® has long represented the reference material against which alternative PEMs are compared.

Despite its widespread use, the commercialization of Nafion® faces a significant obstacle due to its high material and production costs [42], currently estimated at 800 USD/$m^{2,}$ and, in combination with the future restrictions, this makes it necessary to research other routes. A first line of research has focused on reducing the fluorinated content of Nafion®-based systems while preserving their well-established electrochemical performance. In this context, Nafion® has undergone modifications like the blending with other polymers like ionic liquid [43] or achieving multilayered systems [44,45]. It is interesting the addition of nanofillers like, among the others, g-C_3N_4 nanosheets [46], graphene [47,48], silica [49] and zeolite [43] with the aim of improving membrane properties and partially reducing the amount of fluorinated material required. These approaches have often produced promising results in terms of conductivity, mechanical stability, and durability. However, they still rely on PFAS-based architectures and therefore do not fully address the long-term regulatory and environmental concerns associated with fluorinated materials. For this reason, although the modification of Nafion® remains a valuable transitional strategy, the long-term direction of research is increasingly moving toward the complete replacement of PFAS with fluorine-free membrane alternatives.

3.1.2. Low-Temperature Hydrocarbon and Bio-Based PFAS-Free Membranes

Low-temperature PFAS-free proton-conducting membranes represent one of the most actively explored research directions for replacing conventional PFSA-based materials in PEM technologies. Within this group, aromatic hydrocarbon polymers and bio-based matrices have attracted particular interest because they combine the possibility of eliminating fluorinated moieties with tunable proton-conduction pathways, lower material costs, and broad chemical versatility. However, their development is still governed by the need to balance proton conductivity with dimensional stability, mechanical integrity, chemical durability, and suitability under realistic PEMFC or PEMEL operating conditions. For this reason, the following sections examine the main classes of low-temperature PFAS-free membranes, highlighting both their advantages and their current limitations.

Sulfonated Aromatic Membranes

Among low-temperature PFAS-free membranes, sulfonated aromatic polymers are among the most extensively investigated candidates. Their interest arises from the possibility of combining high ion-exchange capacity and relatively good thermal and mechanical resistance with fully fluorine-free polymer backbones.

SPEEK-Based Membranes

Sulfonated poly(ether ether ketone), or SPEEK, membranes are becoming a promising contender to replace Nafion® in PEM. This is because SPEEK offers several advantages: it is mechanically strong, chemically stable, resists methanol effectively, and it is cost-effective. However, a drawback of SPEEK is its high water uptake and swelling considerably when its ionic exchange capacity (IEC) is high (Figure 3).

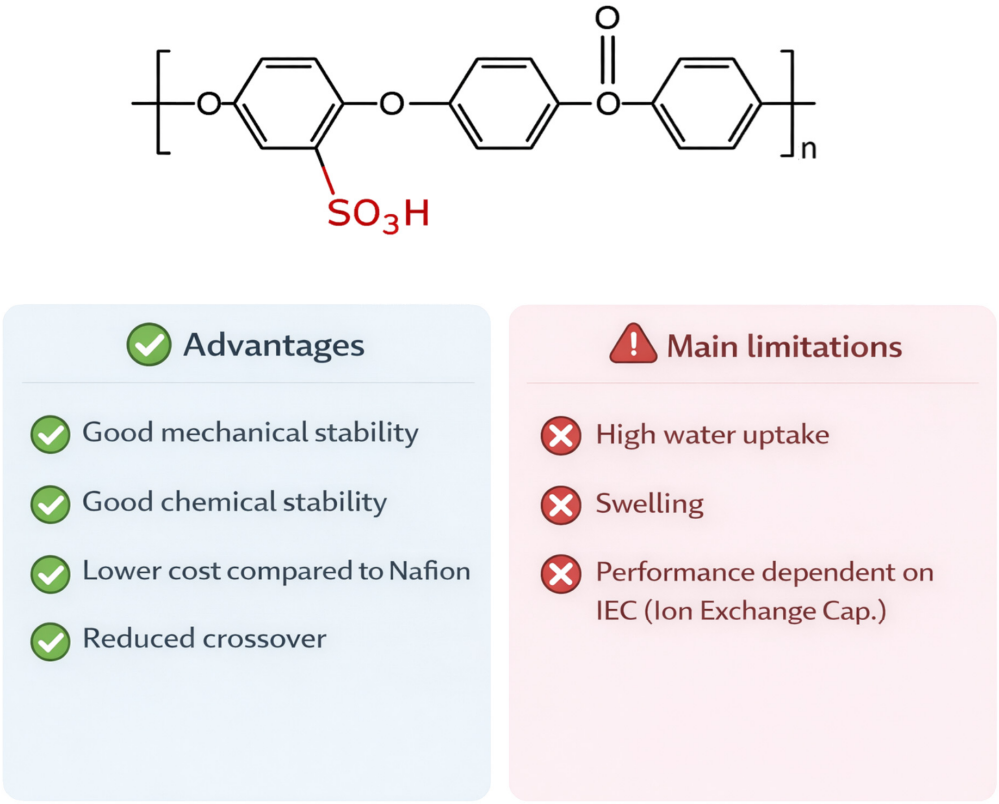


Figure 3. SPEEK chemical structure with example of added sulfonic acid groups highlighted and trade-off between performance advantages and limitations.

Teixeira et al. (2025) [50] reported a series of newly modified SPEEK-based membranes incorporating phosphonic acid dopants, which significantly improved thermal stability, water uptake control, and proton conductivity compared to pristine SPEEK. Although primarily tested in electrochemical cells rather than high-pressure PEMEL setups, these findings confirm the adaptability of SPEEK chemistry and its potential as a PFAS-free alternative for electrolyzer membranes.

Literature underlines how high-performance SPEEK membranes can be improved by introducing cross-linking networks [51,52], thus achieving impressive proton conductivity (up to 417.0 mS·cm^{-1}) and strong tensile strength (120.6 MPa) [53,54]. A composite PEEK membrane was also fabricated using a co-modification method by Chu et al. [55] that achieved a better balance in the conduction performance and mechanical stability. However, the authors did not perform tests for high-pressure conditions. Prepared membranes have enhanced mechanical and chemical durability. Moreover, it is clear that inorganic–

organic functionalization can also enhance the properties of polymers. Sharma et al. [56] synthesized a modified SPEEK PEM via sol–gel organo-silane based for suitability in direct methanol fuel cells. Different concentrations (0.2–1.5 wt%) of APTES are incorporated in SPEEK matrix by in situ sol–gel method. It can be concluded that the 0.8 wt% Si-SPEEK composite membrane has the potential to give effective results in terms of conductivity. Kim et al. [57] investigated the effect of TiO_2 in the addition of SPEEK membrane. The results showed that an appropriate quantity of 15 wt% of anatasium TiO_2 can significantly improve the proton conductivity (which was evaluated to increase from 10.4 $mS{\cdot}cm^{-1}$ to 145.3 $mS{\cdot}cm^{-1}$) and physiochemical properties of the prepared composite membrane, as well as the PEM performance and durability under 20% of relative humidity. Moreover, the power density value is increased to 0.074 W cm^{-2}, compared to bare PEM (0.035 W cm^{-2}). However, when loading 20 wt% of anatasium TiO_2, the aggregation effect tends to produce a decrease in proton conductivity (122.5 $mS{\cdot}cm^{-1}$).

Other Aromatic Hydrocarbon Membranes

While SPAEK-based membranes (Sulfonated Poly(aryl ether ketone)) can be used instead of Nafion® based membranes (Figure 4), tests available have shown SPAEK-based membranes suffer low operational stability and degrade faster than Nafion® [58]. However, 3000 h of operation are reported [59]. This is due to the attack of ·OH radicals on the non-sulfonated phenyl ether aromatic rings, which causes scissions in the main SPAEK chain and results in material degradation [60]. While the stability of Nafion® membranes has been proven to be increased precisely by fluorination of the main-chain phenyl groups [61]. The SPAEK level of dissociation of sulfonic groups is very little compared to Nafion®. This is because its rigid aromatic structure, along with low acidity, results in thinner hydrophilic channels compared to the Nafion®, which creates wider gaps among sulfonic acid functional groups, thus delaying proton transport [62]. However, Egemole et al. (2024) [63] demonstrated that a reinforced sulfo-phenylated polyphenylene (SPP) membrane, a fluorine-free aromatic analogue, achieved high stability and performance in PEM water electrolysis, with significantly reduced hydrogen crossover and a voltage degradation rate of only ~1.5 mV h^{-1}. This evidence indicates that suitable reinforcement strategies can overcome the durability limitations typically observed in SPAEK membranes under electrolysis conditions.

Ko et al. (2023) [64] extended the design principles of aromatic hydrocarbon membranes by synthesizing multi-block copolymers enriched with naphthalene moieties. In PEM water electrolysis tests, these membranes exhibited hydrogen gas barrier properties 3.6 times superior to those of Nafion®-212 and delivered higher current densities, underscoring their potential as PFAS-free, high-performance alternatives in PEMEL systems.

An amino-sulfonic acid–based bi-functionalized metalorganic framework (MOF) consisting of an ionic cross-linking structure in SPAEK was made by Duan et al. [65]. The membrane exhibited excellent proton conductivity of 188 $mS{\cdot}cm^{-1}$ along with a fuel cell power density of 91 $mW{\cdot}cm^{-2}$. This behaviour is related to the high content of amino groups on its surface, which could form more acid-base ionic pairs with the sulfonic acid groups of the resulting sulfonated poly(arylene ether) ketone (SNF-PAEK). Neelakandan et al. synthesized SPAEK composite membrane with surface-functionalized fullerene (through the solution casting method with 0.25–1.0 wt% of s-Fu). BSPAEKS/S-Fu with 0.75 wt% displayed maximum proton conductivity of 322 $mS{\cdot}cm^{-1}$ with fuel cell performance of 74.38 $mW{\cdot}cm^{-2,}$ which is higher than both pristine BSPAEKS and Nafion®-212 membrane. This is due to the addition of s-Fu into the BSPAEKS matrix, providing the additional proton-conduction sites and hydrogen bond formation between the filler and polymer results in better proton-conduction pathways. In addition to that, several researchers have

incorporated different inorganic materials to improve electrochemical properties, such as SiO_2 [66] and TiO_2 [67]. Incorporation of hygroscopic inorganic compounds (e.g., SiO_2, TiO_2, SnO_2, and ZrO_2,) into an organic matrix generally leads to increased water absorption and proton conductivity.

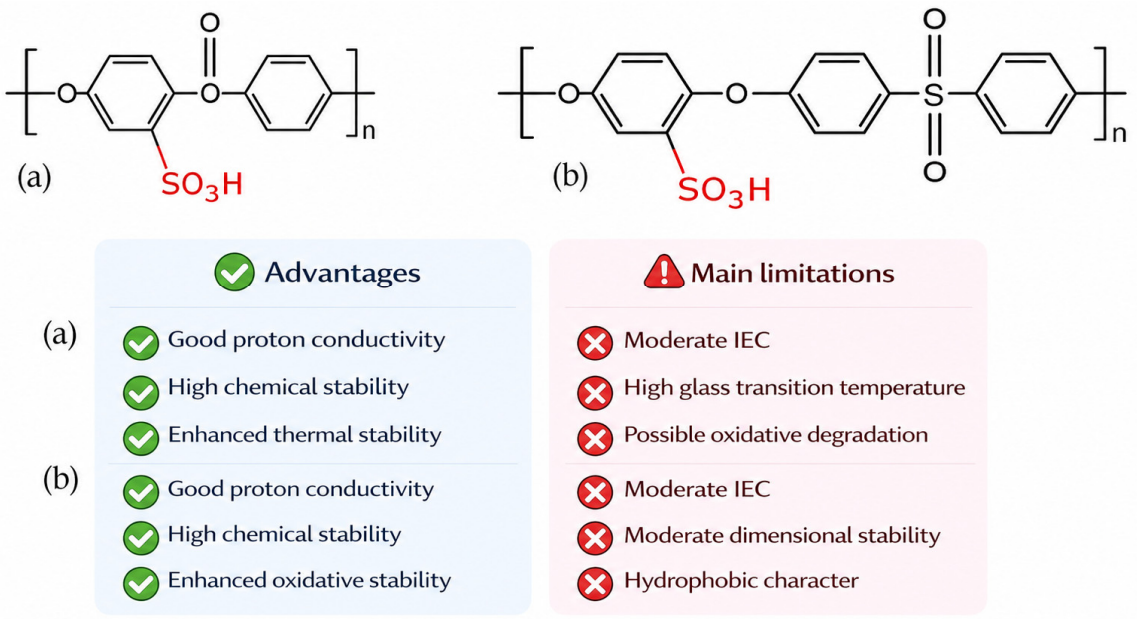


Figure 4. Chemical structures of sulfonated aromatic hydrocarbon membranes: (**a**) SPAEK-type and (**b**) SPAES-type, with example of added sulfonic acid groups highlighted, and trade-off between performance advantages and limitations.

Liu et al. [66] investigated the sol–gel method as an effective approach to introduce hygroscopic inorganic components and cross-linking structure. The advantage of this method is that mild conditions (low temperature and pressure) are used in the processing of membrane preparation. Starting from the sulfonated poly(arylene ether), SPAES-containing 4-animo-phenyl pendant group, a silane coupling agent, (3-isocyanatopropyl) triethoxysilane (ICPTES), and 3-(trihydroxysilyl) propane-1-sulfonic acid (THOPS) were then added. The THOPS was added to react with the amino groups of Am-SPAES (Figure 4) to form a "bridge linkage" between inorganic and organic components. The use of the cross-linker that contains the proton-conducting moiety, such as sulfonic acid-functionalized silica (SiO_2-SO_3H), avoids aggregation of the fillers in the organic matrix. This phenomenon can lead to instability of the entire membrane, as in the case of a directly doping with acid-functionalized filler, where the poor molecular interactions easily cause aggregation of the fillers in the organic matrix. The introduction of SiO_2-SO_3H fillers results in a slightly lower proton conductivity (43.0 mS·cm^{-1}) compared to Nafion® 117 (53 mS·cm^{-1} at 20 °C), but anyway higher than bare SPAES (20.0 mS·cm^{-1}).

Sulfonated Polyimides (SPI)

Sulfonated polyimide (SPI) is revealed to be another promising polymer material for PEM (Figure 5). However, its tendency to hydrolyse in the presence of water provides a significant challenge, as this degradation negatively impacts performance [68].

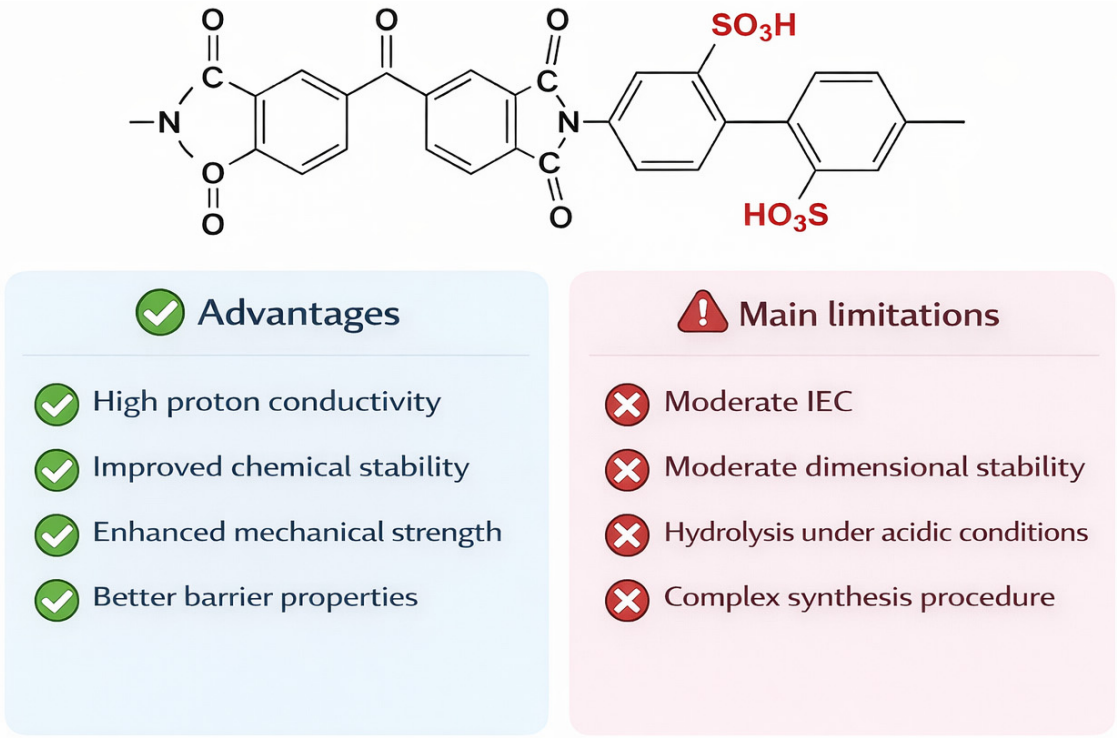


Figure 5. SPI chemical structure with example of added sulfonic acid groups highlighted, and trade-off between performance advantages and limitations.

Afzal and Wang (2025) [69] noted in their review on sulfonated organic polymer membranes for PEM water electrolysis that the hydrolytic instability of SPI represents a major drawback for direct application in PEMEL. They underlined that while SPI membranes can deliver high proton conductivity in fuel cell environments, their durability under liquid water exposure is limited, requiring substantial stabilization strategies before they can be considered viable candidates for electrolysis. Hydrolysis occurs due to the interaction between carbonyl carbon atoms within the membrane and water molecules. Since water is crucial for proton conductivity, preventing this hydrolysis is essential. Researchers are exploring methods to enhance the electron density of these carbon species to improve stability. While progress has been made, further research is ongoing to boost their durability, ideally to levels comparable to Nafion®, without compromising other beneficial characteristics. The review paper of Kausar et al. [70] underlined different strategies to improve membrane stability. This study discussed polyimide and its composite-based membranes. Modified polyimides, such as sulfonated polyimides and the effect of nanofillers (including silica, CNTs, graphene, and titania) on the proton conductivity and water stability, were demonstrated. Hooshyari et al. [71] reported a high-temperature nanocomposite membrane for proton exchange purposes by blending SPI, PBI (polybenzimidazole), and $SrCe_{0.9}Yb_{0.1}O_{3-d}$ (SCYb) perovskites. Perovskites are considered to be one of the fastest proton conductors. The resulting membrane was able to give a proton conductivity of 131 mS·cm^{-1} at 180 °C and 8% relative humidity. The increase in power density from 310 mW·cm^{-2} in PBI-SPI blend membranes (SPI/PBI: 25 wt%) to 590 mW·cm^{-2} in PBI-SPI-SCYb nanocomposite blend membranes (SPI/PBI: 25 wt% and 7 wt% of SCYb) was achieved at 0.5 V, 8% RH and 180 °C. The data underlined how this composite membrane can be used as a high-temperature fuel cell with high proton conductivity. In terms of power density, You et al. [72] obtained an improvement by adding rice husk ash (RHA) as bio-filler in SPI-based membrane. The maximum power density was increased from 8.0 mW cm^{-1} to 13.0 mW cm^{-1} using a composite membrane with 15 wt% RHA. An

effort to improve the weak hydrolytic stability of SPI, a cross-linked SPI with a highly branched main chain (SPI-B), was synthesized via a direct polymerization reaction by Hu et al. [73], using ethylene glycol diglycidyl ether (EGDE) as the cross-linking agent. Compared with the other corresponding membranes, the branched membrane showed enlarged interchain spaces facilitating water uptake, which resulted in a significant improvement of the proton conductivity; although, generally, cross-linked membranes have a depressed molecular motion. Considering that proton conductivity at the highest tested temperature was about 110 $mS \cdot cm^{-1}$ with respect to a non-branched membrane (about 100 $mS \cdot cm^{-1}$), even if compared to Nafion® 212, used as reference membrane, the conductivity was about 150 $mS \cdot cm^{-1}$. The fuel cell power density with the branched SPI-B membrane was 63.4 $mW \cdot cm^{-2}$, which is higher than the 43.0 $mW \cdot cm^{-2}$ of a common cross-linked linear SPI membrane. The thermal stability was not influenced by the highly branched structure, and TGA data underline how the decomposition temperature starts at 200 °C for all the analyzed membranes, branched or not.

SPI-based membranes were employed in the realization of functionalized graphene or GO by Rehman et al. [74]. A sulfonated imidized GO (SIGO) was used to achieve a composite membrane. SIGO content increases proton conductivity by making the dissociation of the hydrated acidic functional groups (SO_3H and COOH) and transport of the hydrated proton easier. The resulting proton conductivity was 112 $mS \cdot cm^{-1,}$ adding 3 wt% of SIGO, and it is improved with respect to the bare NSPI membrane (85 $mS \cdot cm^{-1}$). The Nafion® 117, used as reference material, showed a proton conductivity of 95 $mS \cdot cm^{-1}$. After incorporation of the SIGO in the NSPI matrix, there is a cell performance improvement in comparison with the NSPI membrane with a maximum power density of 74. 9 $mW \cdot cm^{-2}$.

Chitosan and Other Bio-Based Matrices

Natural polymers offer a non-toxic and low-cost alternative to synthetic options like Nafion®. Despite their promising properties, research on natural polymer-based membranes, including those made from cellulose [75], pectin [76], chitin [77], and alginic acid [78], is not widespread. In contrast, chitosan-based membranes have been the subject of extensive research for PEMFC applications. Chitosan (CS) is a biodegradable and non-toxic biopolymer, derived from chitin, a substance found in the exoskeletons of various invertebrates, through a process called alkaline deacetylation.

One of CS's key properties (Figure 6) is its pH-dependent positive charge when dissolved in a solution. This allows it to readily form complexes with negatively charged polymers.



Figure 6. Chitosan trade-off between performance advantages and limitations.

CS shows great promise as a material for PEMs in fuel cells. Its biocompatibility, environmentally friendly nature, and ability to reduce crossover make it an attractive alternative. However, CS (10^{-6} $S \cdot cm^{-1}$) [79] shows a low proton conductivity compared to Nafion® (10^{-4} $S \cdot cm^{-1}$), due to its high crystallinity. The lack of proton mobility in CS

is due to partial protonation of weak alkaline groups in its main chain. Therefore, the conductivity is facilitated through the transport of OH^- across its small amorphous region.

The available literature underlines how proton conductivity was increased by the addition of inorganic fillers. In this regard, Melo et al. [80] recently demonstrated that CS-based membranes reinforced with bamboo-derived nanocellulose and graphene oxide exhibit enhanced mechanical hardness, improved thermal stability, and significantly higher electrolysis performance. The optimized composite reduced the onset voltage for hydrogen production by nearly 0.7 V compared to pristine CS, highlighting how bio-derived PEMs can be effectively tailored for PEM water electrolysis applications. Similarly, Divya et al. [81] showed that the addition of 0.75% MoS_2 gives good proton conductivity of 3.61 $mS{\cdot}cm^{-1}$ along with the highest water uptake and IEC compared to commercial Nafion® 212. Moreover, the hydrophilic nature of the membrane is increased with thermal and chemical stability due to hydrogen bonding between CS and MoS_2.

In the study of Liu et al. [82], silica-coated carbon nanotubes (SCNTs) were obtained by a simple sol–gel method and were utilized in the preparation of CS/SCNTs (CS/SCNTs) composite membranes. The thermal and oxidative stability, morphology, mechanical properties, water uptake, and proton conductivity of CS/SCNTs composite membranes were investigated. Thanks to the hydrophilic silica layer coated on CNTs, the risk of electronic short-circuiting is eliminated, and the interaction between SCNTs and CS is enhanced to ensure the homogenous dispersion of SCNTs, even if there is a reduction in water uptake of CS/SCNTs membranes owing to a decrease in the effective number of the amino functional groups of CS. The CS/SCNTs composite membranes are superior to the pure CS membrane in thermal and oxidative stability, mechanical properties and proton conductivity. The results of this study suggest that CS/SCNTs composite membranes exhibit promising potential for practical application in proton exchange membranes.

3.1.3. Intermediate/High-Temperature Proton-Conducting Membranes

Intermediate-temperature proton-conducting membranes represent a distinct class of PFAS-free materials that should not be directly compared with conventional low-temperature PFSA-based membranes, as they operate under different thermal and hydration conditions. Among the different proton exchange membranes used in high temperatures, those made from polybenzimidazole (PBI) doped with phosphoric acid are the most common (Figure 7). They offer several benefits, such as faster electrochemical reactions, better handling of water, and increased resistance to carbon monoxide contaminants often found in hydrogen fuel cells [83].

Aili et al. [84] demonstrated high-temperature steam electrolysis using phosphoric-acid-doped PBI (but also PFSA/PBI blends), operating at 130 °C. They state stronger polarization curves (≈0.5 A cm^{-2} at 1.75 V) but showed poor durability.

Garbe et al. [85] analyzed thin membranes (≈50 μm) up to 120 °C, quantifying up to ~14% efficiency gains at 3 A cm^{-2} but also reported the need to mitigate mechanical/chemical degradation at high T.

The current literature identified that incorporation of nanofillers into PBI is a straightforward and effective strategy for concurrently enhancing the proton conductivity, mechanical strength, and oxidative stability of PBI membranes [58,86]. Different nanofillers, such as clays, graphene oxide, silicon-based oxides and MOF, have been revealed to be effective in improving membrane properties of HT-PEMFCs. Good dispersion of modified laponite clay, modified using a series of ammonium and pyridinium salts, was realized in PBI, achieved by Placket et al. [87]. The obtained composite membranes exhibited hydrogen permeability ranging from 0.6 to 1.2 × 10^{-10} mol cm^{-1} s^{-1} bar^{-1} from 100 to 200 °C, which is five times lower than that of acid-doped pristine PBI membranes. Ghosh et al. [88]

employed a composite membrane of PBI with reduced graphene oxide (rGO) at an optimum loading of 1%. It is observed that with very low (1%) rGO content, composite PBI membrane (rGO-PBI-1) offers the maximum enhancement of all properties: water uptake, acid uptake, proton conductivity, ion exchange capacity, acid retention capacity, chemical stability, and yield strength.

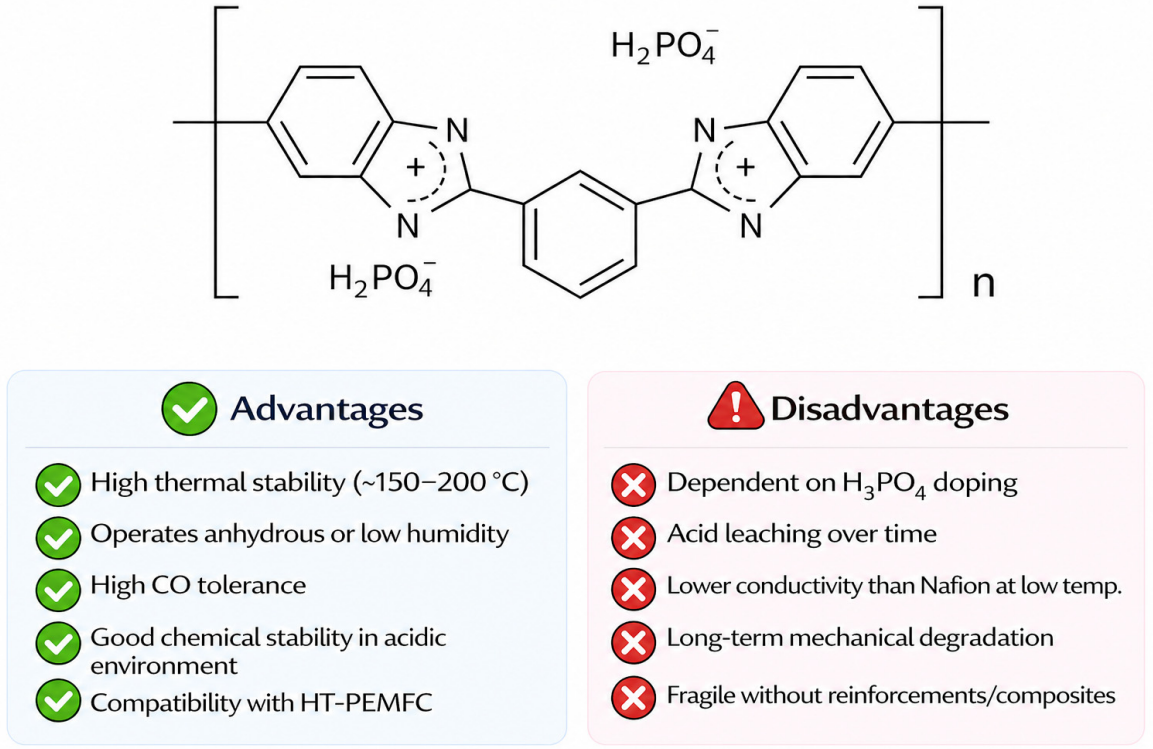


Figure 7. PBI trade-off between performance advantages and limitations.

Sakthivel et al. [89] developed a phosphoric acid-doped blended membrane based on sulfonated poly(1,4-phenylene ether-ether sulfone) (SPEES) and quaternized poly(2,6-dimethyl-1,4-phenylene oxide) (QPPO), in which the synergistic interaction between sulfonic acid groups, quaternary ammonium groups, and phosphoric acid species enhanced proton transport and membrane stability. The optimized SPEES-QPPO-12%/PA membrane reached a proton conductivity of 159.7 mS cm^{-1} at 90 °C and 95% RH, clearly exceeding the pristine SPEES membrane. In single-cell H_2/O_2 fuel cell tests, it delivered a maximum power density of 0.770 W cm^{-2} and a current density of 1.835 A cm^{-2} at 70 °C and 95% RH, compared with 0.243 W cm^{-2} for pristine SPEES and 0.539 W cm^{-2} for Nafion®-212 under the same conditions. The membrane also showed improved durability, maintaining operation for 110 h at 0.4 A cm^{-2}, with a degradation rate of only 0.012 V h^{-1}, whereas pristine SPEES failed after 18 h. These results indicate that phosphoric acid-doped acid–base aromatic polymer blends can significantly improve conductivity, power output, and operational stability, and may therefore represent a promising route for extending hydrocarbon-based PEMs toward more demanding thermal operating windows.

As a concluding remark to Table 1, it is possible to more clearly position the main PFAS-free membrane classes relative to each other, highlighting that none of the currently available solutions fully matches the performance envelope of perfluorinated materials, but rather represents a compromise among proton conductivity, chemical stability, and long-term durability.

Table 1. Key properties, operating windows, durability, and main limitations of representative PFAS-free proton-conducting membranes proposed as alternatives to Nafion®.

Material	Type	σH+ (S/cm)	T Operative (°C)	Stability	Durability	Limits	References
SPEEK	Aromatic sulfonated	0.01–0.2	≤80	Moderate	~1–3000 h	Swelling, radicals	[50–57]
SPAEK	Aromatic sulfonated	0.05–0.3	≤90	Moderate	~3000 h	Brittleness, fast decay	[64–67]
SPI	Sulfonated polyimide	0.05–0.1	≤80 (humid)	Poor hydrolytic	~100 h	Hydrolysis	[68–74]
Chitosan	Biopolymer	10^{-3}–10^{-2}	≤80	Weak acidic	Days–weeks	Low σ, dissolution	[79–82]
PBI/H_3PO_4	Aromatic heterocyclic	0.05–0.07 (150–200 °C)	120–180	High (acid issues)	>20,000 h	Acid leaching, lower ORR	[58,83,87,88]

In general, sulfonated aromatic polymers (SPEEK and SPAEK) emerge as the most mature and balanced alternatives. They provide relatively high proton conductivity (up to 0.2–0.3 S/cm) and benefit from well-established processing routes; however, they are intrinsically limited by swelling phenomena, radical-induced degradation, and backbone instability under realistic operating conditions. While SPEEK offers significant tunability through crosslinking and incorporation of inorganic fillers, SPAEK tends to exhibit faster performance decay and higher mechanical brittleness, making long-term stability a key unresolved challenge.

Sulfonated polyimides (SPI) represent an interesting class due to their initially good conductivity and potential applicability under controlled conditions, but their poor hydrolytic stability constitutes a fundamental limitation. The susceptibility of the imide linkage to hydrolysis leads to rapid degradation (on the order of hundreds of hours), which is incompatible with practical applications unless substantial chemical modifications are introduced.

Biopolymers such as chitosan occupy a different niche altogether. While they offer clear advantages in terms of sustainability, low cost, and non-toxicity, their electrochemical performance remains significantly lower, and their stability in acidic environments is limited to short timescales (days to weeks). As a result, their most promising role lies in composite or hybrid systems rather than as standalone membranes.

Finally, phosphoric acid-doped PBI stands out as the only PFAS-free system capable of approaching Nafion®-like durability (>20,000 h) while operating at elevated temperatures (120–180 °C), offering clear advantages in terms of electrode kinetics and impurity tolerance. However, this system introduces specific drawbacks, including acid leaching and reduced ORR activity, as well as a lower proton conductivity compared to the best-performing low-temperature sulfonated polymers.

Overall, the comparison highlights a fundamental trade-off between conductivity and stability: highly conductive materials (e.g., SPEEK, SPAEK) suffer from durability and chemical stability issues, whereas the most stable systems (e.g., PBI/H_3PO_4) operate in different temperature regimes and introduce additional constraints related to acid management. Emerging solutions, particularly hybrid organic–inorganic membranes developed via sol–gel strategies, aim to bridge this gap by combining high conductivity, chemical robustness, and mechanical integrity within a single architecture; however, they still require significant technological maturation to reach the performance and readiness levels of PFAS-based systems.

3.2. Liquid–Gas Diffusion Layers

Gas diffusion layers (GDL), also called liquid–gas diffusion layers (LGDL) or porous transport layers (PTL) are permeable layers between the catalyst support layer and the bipolar plates, which not only provide the pathway for transporting the reactants/products during the electrochemical reactions, but also electrically connect the membrane–electrode assembly (MEA) and the bipolar plates [90]. Additionally, they ensure efficient delivery of water to the anode and removal of hydrogen and oxygen from the electrodes. When the current density increases, O2 bubbles can block water flow to the catalyst, which may translate into mass transport losses and eventually cell failure [91]. Therefore, maintaining continuous water pathways in the PTL is critical [92]. Furthermore, factors such as pore size, porosity and surface modifications are key for reducing the overpotential and therefore, enhancing PEMEL performance [90].

In a PEMEL, these processes occur under harsh conditions, such as acidic environments (pH < 4) with high overpotentials (~2 V) and the presence of gas, particularly challenging for LGDLs, especially on the anode side, where the medium is highly oxidizing due to the presence of O_2 [93]. Furthermore, the porosity of the LGDL material is crucial for its functionality; in general, low porosity can hinder water and gas transport, while higher porosity aids gas evacuation but increases ohmic losses at LGDL-MEA and LGDL-bipolar plate interfaces. Sintered Ti at a high temperature from powders, Ti mesh or Ti foams are commonly used materials in this application, particularly on the anode side, due to the harsh conditions. The existing pores facilitate gas and water flow while providing a large contact area with the electrodes, enhancing conductivity despite introducing higher resistance in the cell's acidic environment [90].

The conditions on the cathode side of a PEMEL are not as extreme, and the cathode LGDLs can be made of carbon fibre paper or felt, with the advantage of being more cost-effective materials. These LGDLs typically incorporate PTFE (polytetrafluoroethylene), which serves as a hydrophobic agent and, depending on the LGDL type, also functions as a binder. This hydrophobic treatment is crucial for efficient water management and proper cell operation [24]. Optimization of the PTFE coating is critical, as it can affect the microstructure of the LGDL by reducing the porosity and altering the pore size distribution, the gas diffusivity, and permeability (due to loss of pore volume), as well as decreasing the electrical conductivity by increasing the contact resistance [94]. Additionally, replacing PTFE is desirable to enhance the sustainability of both the LGDLs and the overall PEMEL system. While alternative coatings have been extensively studied for PEM fuel cell (PEMFC) applications [95–98], research specific to PEM electrolyzers (PEMEL) remains limited.

Yoon et al. [95–97] have conducted studies in which carbon LGDL for PEMFC coated with the typical PTFE was replaced by a fluorinated silane ((hepradecafluoro-1,1,2,2-tetrahydrodecyl)triethoxysilane, HTTS). The coating was applied by dip-coating, and the samples were heat-treated at 200 °C for 30 min (in contrast to the PTFE, which was treated at 350 °C for 30 min). Coatings were evaluated in terms of hydrophobicity (water uptake and water contact angle), durability (long-term vibration test), gas permeability, and surface electronic resistance. The results showed that the HTTS-coated carbon paper was very thin and uniform, which resulted in a bigger pore size and better gas permeability values as well as surface electronic resistances, than those of the PTFE-coated carbon paper. Despite these promising results and the improved sustainability, HTTS still relies on fluorine for hydrophobicity.

In contrast, different studies have shown good behaviour of PDMS (polydimethylsiloxane-based)-coated LGDL [96–98]. Wang et al. [98] studied a coating comprising a mixture of silica and PDMS as a replacement of PTFE for carbon LGDL for PEMFC, and results showed higher hydrophobicity and better performance than conventional LGDL and PTFE-coated

LGDL. Sun et al. [96] studied a carbon LGDL that was coated with a mix of PDMS and carbon black at different concentrations and compared it to the commercial one coated with PTFE. The work showed that the obtained hierarchical micro-nanostructure resulted in a superhydrophobic surface with high durability, showing low corrosion current density. In the study conducted by Öztürk et al. [97], it was shown that by combining PDMS with silica particles, the surface of the LGDL was more hydrophobic and the PEMFC performance was improved, especially at high humidity levels.

In summary (Table 2), LGDLs play a crucial role in PEMEL, facilitating reactant transport and electrical connections. To improve their performance, researchers have been studying alternative hydrophobic coatings to replace polytetrafluoroethylene (PTFE). Studies have shown promising results using polydimethylsiloxane-based (PDMS) coatings, which offer improved sustainability and hydrophobicity. These coatings enable better gas permeability, surface electronic resistance, and durability. Although these PDMS-based coatings show significant potential, they have not yet been fully characterized for commercial use. Moreover, all existing studies have focused on PEMFCs, leaving a gap in research for PEMEL applications. Further investigation is needed to develop PTFE alternatives that meet all performance requirements for PEMEL systems.

Table 2. Summary of PFAS-based and emerging PFAS-free hydrophobic coatings for LGDLs, emphasizing performance trade-offs, sustainability aspects, and current limitations for PEM electrolyser applications.

Coating	PFAS-Free	Hydrophobicity	Stability	Key Advantages	Limitations
PTFE	✕	High	High	Benchmark	PFAS
HTTS	✕ (fluorinated)	High	Good	Thin coating, permeability	Still PFAS
PDMS	✓	High	Good	Sustainable, tunable	Limited PEMEL data
PDMS + silica	✓	Very high	Improved	Superhydrophobic	Scale-up unknown

3.3. Sealings and Gaskets

In PEM devices, gaskets and sealings are the key components that have to ensure gas tightness, electrical insulation between bipolar plates, and long-term stack stability. They must face compression, cyclic temperature and humidity, and prolonged exposure to acidic and/or oxidizing media, and at the same time maintain unchanged low compression set and adequate mechanical strength.

In current commercial PEM fuel cells and electrolyzers [99], generally, the gaskets are based on three types of elastomer families: fluoroelastomers (FKM and FFKM) [100], ethylene-propylene-diene monomer (EPDM) [101], and silicone rubbers [102]. A comparative overview of the main elastomeric materials currently employed for sealing applications in PEM systems is presented in Figure 8, where their key advantages and limitations are summarized in relation to operating conditions and sustainability constraints.

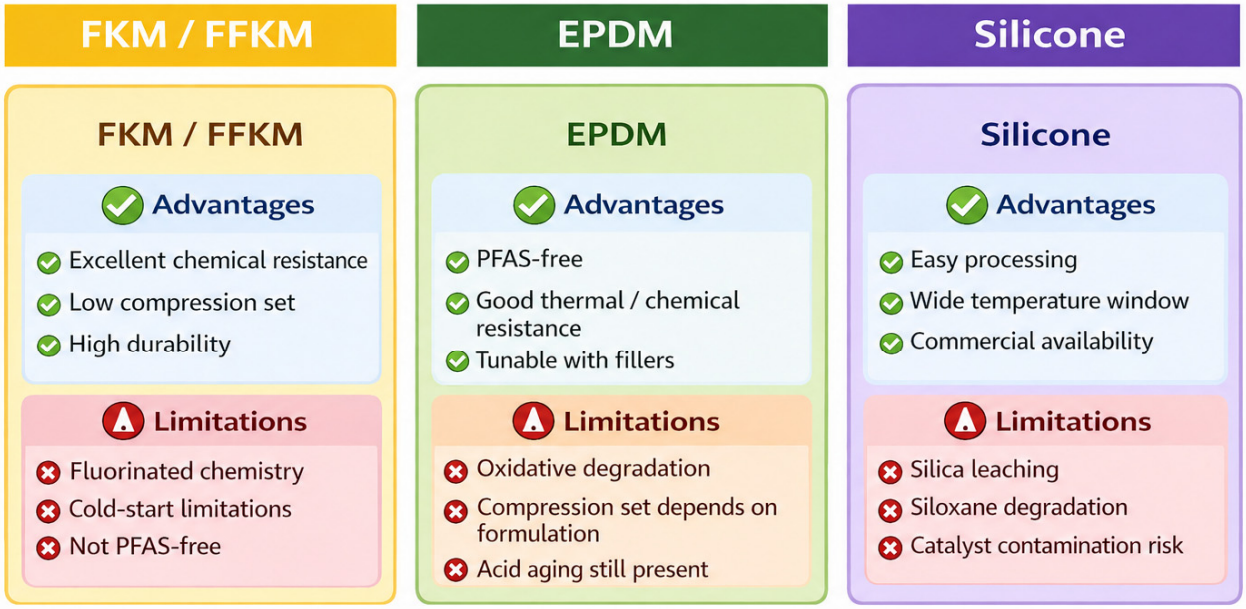


Figure 8. Comparative assessment of elastomeric gasket materials for PEM electrolysis applications, highlighting advantages and limitations of fluoroelastomers (FKM/FFKM), EPDM, and silicone-based materials.

3.3.1. Fluoroelastomers (FKM/FFKM): High-Performance Sealing Materials with PFAS-Related Limitations

Fluoroelastomers (FKM) and perfluoroelastomers (FFKM) are currently used in PEM technology. Their impressive performance, due to fluorine presence in their backbone, ensures low compression set and stable mechanical properties over a wide range of operative conditions [103].

Commercial FKM typically shows a good elasticity with a very low compression set, around 2–3% [104] and low gas permeability [105]. Many KFM tolerate long-term contact with acidic solutions up to 300 °C [106], while their lower operating temperature is usually close to −20 °C [107]. On the other hand, they show degradation in strongly alkaline media: tests in 10% NaOH at 80 °C show significant deterioration of commercial FKM grades such as Viton® A, even at early exposure times [108].

Regarding the durability, Tan et al. (2007) [109] studied commercial FKM (Viton® A) in two aqueous sulfuric acid/fluoride electrolytes: an accelerated durability test solution and a solution like real PEM operating conditions. Tests at 60 and 80 °C for up to 45 weeks showed only mild surface roughening and limited mass change. Lin et al. (2011) [110] extended immersion tests to less than 63 weeks in similar electrolytes and reported that FKM had the lowest weight loss among the rubbers studied, again confirming its superior chemical stability.

Qiu et al. (2020) [111] deepened the mechanical response of FKM under compression. They found that it shows small stress variations (<0.4 MPa) over a wide compression range, indicating a relatively broad window of stable sealing force. They also showed that, at 100 °C, FKM stiffness decreases and the seal-contact stress drops under constant strain, pointing to a loss of sealing force under high-temperature operation.

Temperature variations can also reduce FKM sealing performance. Derham et al. (1997) [112] measured the sealing force as a function of temperature and observed an approximately 50% decrease when FKM gaskets were cooled from 80 °C to 23 °C, which they attributed to thermal contraction and thermodynamic effects. Combined with a glass-transition temperature near −20 °C, this makes FKM less suitable for cold-start conditions, although it remains highly robust at intermediate and high temperatures.

3.3.2. EPDM Rubber: A Promising PFAS-Free Alternative with Balanced Performance

Conversely, EPDM and silicone rubbers are hydrocarbon- or silicon-based materials that can be formulated without PFAS. They therefore represent the main non-fluorinated gasket candidates, even though each has disadvantages in terms of durability, leaching, and mechanical retention.

EPDM is a saturated and non-polar elastomer, with unsaturation confined in the lateral chain. These properties allow an excellent heat and weathering resistance, combined with a good resistance to water [103]. Moreover, its low crystallinity allows the introduction of various types and quantities of fillers, useful to tune its properties [113].

EPDM can maintain its mechanical properties up to a temperature of −40 °C [114] and shows good resistance to thermal ageing. A study on EPDM aged for 63 weeks at 80 °C [109] reported only limited variation in dynamic mechanical properties, confirming its usability in long-term equipment.

Moreover, this polymer can be vulcanized via sulphur or peroxide (Figure 9). For the use of interest, the peroxide path is preferred, because it guarantees an improved heat resistance and lower compression set compared to the sulphur path [103].

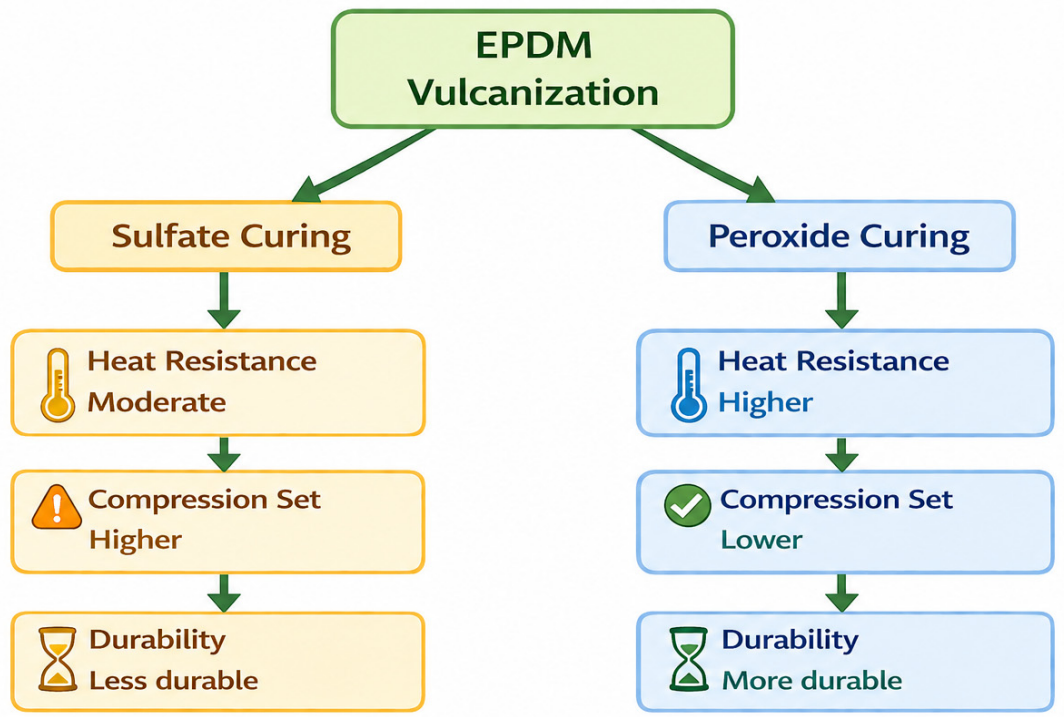


Figure 9. EPDM vulcanization routes: sulphur curing versus peroxide curing, and their resulting effects on thermal resistance, compression set, and durability.

Unfortunately, it is not free from signs of degradation in strong acid media. Mitra et al. (2004) [108] exposed two EPDM grades, with different molecular weights and degrees of branching, to a solution of Cr(VI) oxide and H_2SO_4 with a pH < 1 for up to 12 weeks. Microhardness decreases of 3–4 units in the first 7 weeks.

In typical PEM condition, the EPDM shows a better behaviour: immersed in a solution that mimic the typical one of an operative stack at 23 and 80 °C for 180 days, it demonstrated essentially an unvaried tensile strength of 9 MPa for the printed one, and a slight decrease from 6 to 4 MPa for the sheets, while the compression set remained quite low [115].

The main degradation reasons depend principally on oxidative scission of the chain, decrosslinking until the formation of superficial cracks that diminish the mechanical re-

sistance and dimensional stability. To face this mechanism, the possibility of fillers has been investigated.

Peroxide-vulcanized EPDM with nano-sized carbon black (≈44 nm, from 0 to 60 phr) has been exposed to an acidic solution (pH near 3.5) at a set temperature of 80 °C for 400 and 800 h as an accelerated durability test [116]. The Shore A hardness increased from 51 to 72 (in accordance with ASTM D2240 (https://store.astm.org/d2240-15r21.html, accessed on 14 April 2026)) as the filler content increased from 0 to 60 phr, and the tensile strength increased dramatically from 2.51 to 34.8 MPa before ageing. At the same time, an increase in compression set was also found, reducing the elastic recovery ability under compression. Notably, after ageing, the changes in strength were limited. A formulation with 20 phr of CB offered the best compromise, with hardness ≈ 63, compression set ≈ 2.95%, tensile strength ≈ 11.3 MPa, and modulus at 300% ≈ 3.08 MPa, and it has been proposed as a high-performance gasket material for PEM.

EPDM/silica composites (silica from 0 to 100 phr) have been studied primarily in connection with high-pressure hydrogen applications, relevant to fuel cell vehicles and refuelling stations [117]. At ambient temperature, the H_2 permeability passed from 24.1 to 11.4 fmol·m^{-1}·s^{-1}·Pa^{-1} for 100 phr of silica. This is addressed to a more torturous path imposed by the inorganic fillers. The tensile strength increases until a silica content of 60 phr, after which agglomeration and dilution lead to a decline. After exposure to high-pressure hydrogen, composites with more than 60 phr of silica showed negligible changes in volume, residual hydrogen content, and tensile properties, indicating higher blister resistance and lower hydrogen uptake compared to unfilled.

3.3.3. Silicone Rubbers: High Thermal Stability with Durability and Leaching Constraints

Silicone rubbers are another material widely used as a gasket in PEM devices: they are very easy to process, have a good commercial availability and a proven stability over a large span of temperature. Their heat resistance is correlated to the high bond energy Si-O-Si of their backbone, which admits a maximum operative temperature of 316 °C [106] and flexibility down to −50 °C [103].

From a mechanical standpoint, raw silicone rubbers are extremely weak (tensile strength ≈ 0.34 MPa), so rubbers used industrially as gaskets are heavily reinforced with silica to achieve tensile strengths up to ~17 MPa [103].

Moreover, a long-term exposure to acid and aqueous media typical of a PEM reveals significant weaknesses. In real and simulated conditions, the silicone gaskets face simultaneously mechanical compression, temperature cycling, and aggressive aqueous solutions.

Several accelerated ageing studies have shown that silicone rubbers undergo chemical decomposition of the siloxane structure, together with leaching of silica fillers and other inorganic additives [109,118].

Wu et al. (2020) [118] studied the degradation of a silicone rubber under temperature cycling ranging from −20 to 90 °C, after pre-ageing in a pH 3.35 solution. It has been found that increasing the number of thermal cycles slightly increases the hardness but decreases the sample mass. SEM inspections reveal the formation of surface cavities that evolved into larger voids, compatible with consistent filler detachment and progressive matrix embrittlement.

In PEM application, the same silica network that provides reinforcement is also the main source of contaminant species: silicon-containing species released from the gasket can migrate into the membrane–electrode assembly, alter wettability, and poison the platinum catalyst, reducing fuel cell performance [103,109,119,120].

A promising strategy to mitigate this problem is to modify the surface of the silica filler with silane coupling agents, with the scope to improve its compatibility with the silicone

matrix and reduce the solubility of silica in aqueous media. Sim et al. (2024) [121] studied three coupling agents, methyltrimethoxysilane (MTMS), vinyltriethoxysilane (VTES), and (3,3,3-trifluoropropyl)trimethoxysilane (TFPTMS) at different loadings (Sim et al.).

An increase in their quantities has the effect of reducing tensile strength, elongation at break, and hardness, as the residual low-viscosity silane behaves like a plasticizing silicone oil. On the other hand, the leaching decreases from approximately 65.5 $mg \cdot L^{-1}$ to 4.6 $mg \cdot L^{-1}$ when the silica was treated with the highest fraction of TFPTMS, which reintroduces fluorine inside the gasket. Non-fluorinated silanes (e.g., MTMS, VTES) offer a compromise: they improve filler–matrix adhesion and reduce leaching, but they are less effective than TFPTMS.

Ultimately, a comparison of silicone rubbers, fluoroelastomers, and EPDM in acidic solutions provides a consistent picture: fluoroelastomers are the most chemically and mechanically stable, maintaining tensile strength and low compression set values even under accelerated ageing conditions; silicone rubbers are the ones that suffer the most significant damage, with significant silica leaching, increased modulus, and crack formation; EPDM falls in the middle, with measurable chemical and mechanical ageing that can be mitigated through peroxide vulcanization and the use of appropriately selected fillers. From a stack design perspective, compression set and long-term stability under compression remain the key parameters, along with compatibility with PFAS-free requirements.

Ultimately, Table 3 provides a comparative summary of both the qualitative aspects and some typical value ranges for the three elastomeric systems, specifically for PFAS-free PEM stacks. Fluoroelastomers (FKM/FFKM) remain the benchmark materials from a purely functional perspective, as they combine outstanding acid resistance, low compression set, and very good long-term mechanical stability over a broad operating range. However, their fluorinated nature makes them incompatible with the objective of developing genuinely PFAS-free PEM stacks. Silicone rubbers, by contrast, offer the widest temperature flexibility and excellent low-temperature behaviour, but their practical use is limited by chemical degradation, silica leaching, and the associated risk of contamination of adjacent electrochemical components. EPDM appears to represent the most balanced solution among the currently available PFAS-free candidates: although its resistance in aggressive acidic environments and its compression set are more formulation-dependent than in FKM, these properties can be significantly improved through appropriate peroxide vulcanization and filler optimization. Taken together, these observations indicate that EPDM should presently be regarded as the most realistic baseline material for PFAS-free gasket development, while silicone rubbers may still find use in selected locations where flexibility and processing advantages are particularly valuable. In this sense, the future development of gasket materials for PFAS-free PEM stacks will not depend on identifying a single universal substitute, but rather on tailoring elastomer formulation and stack integration strategy to the specific chemical, thermal, and mechanical demands of each sealing function.

Table 3. Qualitative and quantitative comparison of FKM, EPDM and silicone rubber as gasket materials.

Property/Constraint	Fluoroelastomers (FKM/FFKM)	EPDM	Silicone Rubbers
Resistance to acids	Excellent (ADT, pH ≈ 0–3.5, up to ≥45–60 weeks) [109]	Good (ageing manageable) [115]	Moderate to poor (severe degradation and leaching) [117]
Long-term mechanical stability	Very good (σ_t retained, low stress relaxation) [104]	Good (sensitive but improvable with fillers) [111,116]	Decreasing (modulus increase, embrittlement) [103]

Table 3. *Cont.*

Property/Constraint	Fluoroelastomers (FKM/FFKM)	EPDM	Silicone Rubbers
Useful temperature window	≈−20 to 100–300 °C (depending on grade)	≈−40 to 180 °C [114]	≈−50 to 316 °C [106]
Low-temperature/cold-start behaviour	Critical (Tg ≈ −20 °C, strong loss of flexibility) [107]	Fair [121]	Excellent [106]
Leaching/contamination	Low [103]	Low (data still limited) [103]	High (silica, silicon species) [103]
Presence of fluorine/PFAS	Yes (fluorinated backbone)	No	No in the backbone, yes if fluorinated silanes (e.g., TFPTMS) are used [120]
Cost	High [103]	Low–medium [103]	Medium [103]
Role in a PFAS-free stack	Benchmark only, not acceptable as a gasket material	"Baseline" candidate	Complementary candidate for specific locations
Typical compression set (%)	≈2–3 [104]	≈3–16 (optimisable with peroxides + fillers) [110]	≈28 [114]
Typical hardness (Shore A)	≈55–90 [104]	≈59–64 (higher with fillers) [114]	≈42 (standard reinforced formulations) [114]
Typical tensile strength σ_t (MPa)	≈2 (gasket-type formulations) [104]	≈6.2–9.5 (up to ≈30–35 with optimized CB loading) [114]	≈0.34 (unfilled)–≈17 (heavily silica-reinforced) [106,114]
Hydrogen barrier properties (qualitative indication)	Low permeability (quantitative data limited) [105]	Permeability is reduced with filler [116]	Permeability poorly documented under PEM conditions [122]

3.4. Bipolar Plate

In PEM devices, the bipolar plate (BPP) is more than a simple structural element; it is the bridge that links the cells of a stack, avoiding the mixing of their internal media and collecting their current. Moreover, they separate physically adjacent cells, ensure a controlled distribution of the water and gas, help the heat removal, and give the seal and mechanical integrity of the stack.

For all these reasons, a BPP must combine high chemical stability, high electrical conductivity (low interfacial contact resistance, ICR), good mechanical resistance and suitable surface wettability.

Among the possible materials, traditional graphite meets most of these requirements, especially chemical stability over time, but unfortunately, in exchange, it is permeable to gases, and its production is complex and expensive [123].

On the other hand, bare stainless steel is economic, processable, and compatible with common forming and stamping processes. However, in contact with strong acid electrolytes, it tends to passivate rapidly, to corrode easily and to release metallic ions. For these reasons, to meet its strengths with the harsh PEM media, it is necessary to use coatings that are both protective and conductive [124,125].

An important aspect of PFAS-free chemistry is that the BPP coating can be designed with these qualities without the use of fluoropolymers (Figure 10). In the literature [125,126], different materials have been explored on titanium or steel substrate at the operative condition of a PEM: amorphous carbon or diamond-like carbon (DLC) films, conductive nitrides, carbides, borides, and MAX-phase ceramics are all intrinsically PFAS-free from a compositional point of view.

Among them, the amorphous carbon (a-C) represents a versatile solution. If rightly engineered, it is not only a coating easily to deposit, but it also increases ICR and corrosion resistance. The co-doping with Cr/Ti allows the formation of a percolating nanophase inside the carbon matrix, increasing the sp^2 hybridized fraction and leading to a low ICR with extremely low corrosion rates. Mi et al. (2023) [127] reported a value of ICR on AISI 316L of 3.1 mΩ cm^2 at ~1.4 MPa and a corrosion current of ≈5.7 × 10^{-8} A cm^{-2}, indicating

a process window in which electrical and durability performances are both good. Moreover, the possibility of co-doping with nitrogen and multilayer structure [128] (e.g., a-C/CrN/Ti) has been studied, to tune the balance among conductivity, adhesion to the substrate and corrosion resistance.

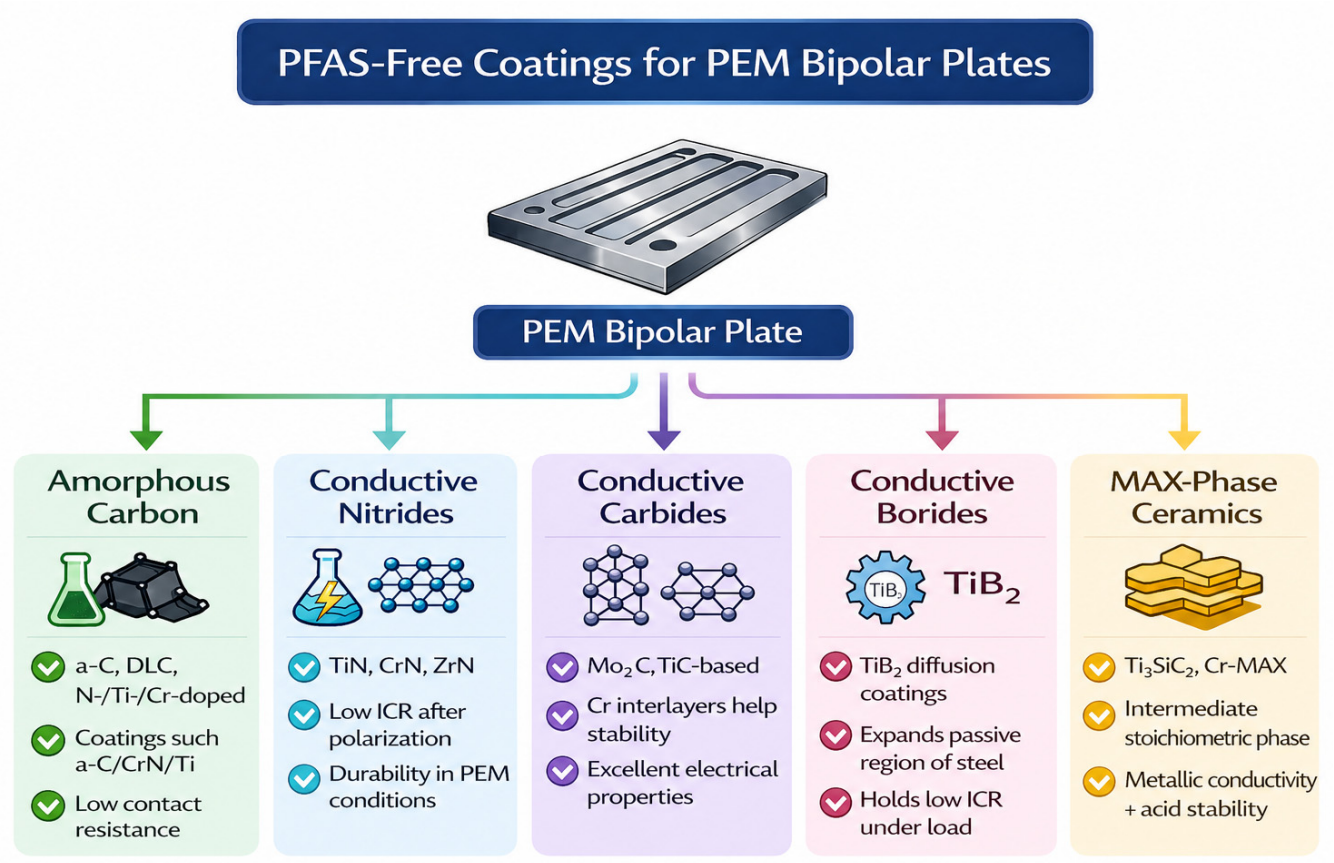


Figure 10. Main PFAS-free coating families for PEM bipolar plates.

Extensive work on these materials shows that the chemistry of the coating is important, as well as other process parameters. The quantity of pinholes and macro-defects, the use of metallic interlayers (Cr/Ti) for adhesion and electron continuity, and the tuning of thickness and/or roughness have been proven to be decisive [125].

A promising strategy is to combine an underlayer of TiN with an a-C top-layer, exploiting the synergic contribution of the two phases. TiN provides a good corrosion barrier and a stable conductive base, while amorphous carbon helps to further reduce ICR and modulate wettability, often making the surface more hydrophobic.

Huang et al. (2023) [129] have proven that the current applied to the carbon target during the deposition has an influence on the a-C microstructure, with an effect on ICR and wettability. Independently, optimized TiN monolayers can ensure low ICR with sub-μA cm^{-2} corrosion currents in sulfuric-acid/trace-fluoride electrolytes near 70 °C [130,131].

Another element that is often underestimated is the manufacturing sequence: the choice between form-then-coat (first shape the plate and then cover it) and coat-then-form (first cover the plate and then shape it) has an impact on the effective contact areas and the tensional state of the coating. Several studies on multilayers of TiN, CrN and ZrN show that the forming/deposition sequence can significantly modify the final ICR, both due to microfracture or cracking of the film during forming, and to the variation in the actual contact area under load [132,133].

Within the family of conductive nitrides, ZrN has emerged as one of the most interesting candidates. It has the capacity to keep low ICR also after long-term polarization

and increase the hydrophobicity. Xu et al. (2015) [126] demonstrate that nanocrystalline ZrN on 316L offers stable behaviour against corrosion and low contact resistance in PEM conditions. Following studies on CrN/TiN [132] underline the importance of controlling the thickness and the micro-failure to keep at minimum the ICR and prevent preferential corrosion paths.

Conductive carbides and borides also represent a very promising class of PFAS-free coatings. Mo_2C film deposited by magnetron sputtering shows a clear beneficial effect from the thickness increase on the ICR, enhanced also by the introduction of a thin Cr interlayer (~100 nm). In a replica of PEM media, Wang et al. (2019) [134] reported for a Mo_2C of about 1.05 µm an ICR of ~7.9 mΩ cm^2, which drops to ~6.5 mΩ cm^2 when the Cr interlayer is present, with a stable behaviour even after corrosion tests. This confirms the idea that modifying the chemistry of the grain boundary of carbides (as in the case of TiC) is an important aspect for co-optimizing passivation capacity and electronic conduction.

Hard borides offer another interesting route. TiB_2 diffusion-type coatings on AISI 304 can expand the passive region of the steel, reduce the corrosion current by orders of magnitude vs. bare steel, and hold ICR $\approx$ 19 mΩ cm^2 at 150 N cm^{-2} even after corrosion exposure. This combination of chemical inertia and conductivity makes TiB_2 a pragmatic hard-ceramic candidate for long-life BPPs [135].

Finally, MAX-phase ceramics offer a particularly interesting hybrid route because they can combine metallic-like conductivity with ceramic corrosion tolerance. Ti_3SiC_2 coatings on stainless steel show low contact resistance and promising durability in simulated PEM media [136]; while Cr-containing MAX phases are being explored to give ICR and acid stability [137].

In summary, these results show that a BPP, appropriately coated with carbon, nitride, carbides, boride, or MAX phase systems, can fully meet the requirements for conductivity, durability, and stability in a PEM environment without relying on fluoropolymers. The challenge is no longer "finding" suitable materials but rather optimizing coating processes and architectures to ensure low ICR, absence of critical defects, and costs compatible with large-scale production of PFAS-free stacks.

4. Key Challenges for PFAS-Free PEM Technologies

4.1. Stability and Durability Under Realistic Conditions

Despite promising advances, PFAS-free materials for PEM fuel cells and electrolysers still face significant difficulties in real-world operation. One of the hardest challenges is achieving chemical and mechanical stability comparable to PFAS-based components under harsh conditions (high voltage, cycling, impurities, etc.). Hydrocarbon ionomers have historically suffered from faster chemical degradation and membrane swelling, leading to shorter lifetimes than perfluorinated Nafion® [138]. The mechanical durability problem is closely related: PFAS-free membranes often exhibit greater swelling and weaker mechanical strength when hydrated/dried, risking tears or gas leaks over time [139]. Reinforcement strategies (e.g., incorporating inert supports) are being studied to address this, but long-term durability in full cells remains an open question [138,140].

4.2. System Integration and MEA Redesign

A second major challenge is the integration of fluorine-free materials into the full system architecture. New membranes and ionomers are rarely drop-in replacements; their different properties (water uptake, gas permeability, thickness, etc.) demand redesign of cell components and operating strategies [141]. For instance, hydrocarbon membranes often require higher ion exchange capacity to achieve similar conductivity, which can alter water management and electrode interface behaviour [142]. For instance, using a

hydrocarbon membrane with a conventional PFAS-based catalyst layer can cause interfacial incompatibilities—one study found that a PFAS binder on a hydrocarbon membrane led to poor performance and eventual delamination of the catalyst layer within 90 h [143]. This illustrates that membrane–electrode interfaces must be re-optimized when chemistries change. Engineers may need to adjust catalyst layer formulations, hydration management, flow field designs, or sealing gaskets to accommodate these alternative materials. Hydrocarbon membranes also typically require a higher ion-exchange capacity (more acid sites per gram) to achieve similar proton conductivity to PFAS [143]. This can alter water management and electrode kinetics, for example, hydrocarbon ionomers with high water uptake might flood electrode pores unless the ionomer content in the catalyst layer is reduced [25]. In short, the entire membrane–electrode assembly design may need tuning. Manufacturing processes likewise may need adaptation. PFAS-free polymers can behave differently during electrode deposition or hot-pressing [144]. Ensuring compatibility of new polymers with existing stack fabrication (e.g., roll-to-roll membrane casting, catalyst ink formulation, sealing techniques) is non-trivial and may require new process parameters. In summary, PFAS-free components introduce system-level integration challenges: one cannot simply swap Nafion® for a new polymer without rethinking the cell design and assembly.

4.3. Lack of Standardized Testing Protocols

A third challenge is the lack of standardized test protocols to evaluate these emerging materials' durability and performance. Currently, different labs use disparate conditions and accelerated stress tests to assess the "lifetime" of PFAS-free membranes, making it difficult to compare results across studies. Researchers and regulators are increasingly recognizing the need for harmonized testing [145,146]. Without standard protocols, claims of improved longevity or efficiency are hard to validate or translate into industry practice. An urgent task is to develop common methodologies (for example, for chemical stability accelerated tests, mechanical cycle tests, and leachate analysis to detect any degraded byproducts) so that data from different groups can be directly compared. In summary, ensuring stability under realistic operating conditions, integrating new materials into complex assemblies, and developing common validation benchmarks are pressing challenges on the path to PFAS-free fuel cells and electrolysers.

5. Emerging Opportunities and Industrial Perspectives

Despite the challenges, the drive toward PFAS-free fuel cells and electrolysers presents rich opportunities, especially for Europe. One major opportunity is the European technological leadership in sustainable hydrogen technologies. The European Union's proactive stance on phasing out PFAS (part of its broader Green Deal chemicals policy) is effectively pushing academia and industry to innovate earlier than in regions with looser regulations [25]. This head starts in developing high-performance PFAS-free materials, which could give European companies a competitive edge in the burgeoning fuel cell and electrolyser market. Substantial public funding is being devoted to this effort—for example, the Horizon Europe Clean Hydrogen program has launched dedicated projects (FASTCH2ANGE, SUSTAINCELL, etc.) to pioneer fluorine-free membranes and components. These initiatives not only aim to solve technical problems, but also to cultivate European expertise and IP in next-generation electrolyser technology. If successful, Europe can supply home-grown solutions to a global industry that will increasingly demand PFAS-free systems, thereby capturing new markets and jobs. Early leadership here aligns with Europe's ambition to set global standards for sustainable technologies (much as it did for auto emissions or renewable energy integration). Another opportunity is preparedness for forthcoming PFAS regulations, which are poised to become more stringent worldwide.

The EU is currently evaluating a sweeping proposal to heavily restrict PFAS across all sectors [17]. By investing now in PFAS-free alternatives, the hydrogen sector can future-proof itself against regulatory shocks. When PFAS bans or heavy penalties come into force, those with ready alternatives will seamlessly continue operations, whereas others may face supply disruptions or forced technology retrofits. In this sense, developing PFAS-free membranes and components is a risk mitigation strategy: it ensures the momentum of hydrogen technologies (fuel cells in transport, electrolysers for green H_2) is not derailed by environmental regulations. Moreover, it positions the industry to meet customer and societal expectations for "zero pollution" clean energy devices. An electrolyser or fuel cell that is not only zero-carbon in operation but also free of "forever chemicals" in its construction offers a compelling sustainability narrative and could become a preferred choice for climate-conscious investors and buyers. In sum, Europe's vigorous push for PFAS-free fuel cells and electrolysers, driven by policy and supported by R&D, offers the twin opportunities of industrial leadership and regulatory readiness—reinforcing the continent's role at the forefront of sustainable innovation.

6. Conclusions

PFAS-containing polymers have been ubiquitous in state-of-the-art PEM fuel cells and electrolysers—used in proton exchange membranes and ionomer binders, as well as in gaskets and hydrophobic gas diffusion layers. While these fluorinated materials impart outstanding chemical stability and proton conductivity, their extreme persistence in the environment is a major concern [145]. Accordingly, impending regulatory pressure (notably a proposed EU-wide restriction on PFAS) is driving an urgent need for viable PFAS-free substitutes in these devices [147]. In response, a wide range of fluorine-free membrane materials have been explored, and many show promising electrochemical performance. These include hydrocarbon-based sulfonated polymers—for example, sulfonated poly(ether ether ketone) (SPEEK), sulfonated poly(arylene ether sulfone/ketone) (SPAEK/SPAES), and sulfonated polyimides (SPI)—as well as other polymer classes like polybenzimidazole (PBI), poly(vinyl alcohol) and even bio-based matrices (e.g., chitosan). Composite and hybrid approaches are also emerging, such as organic–inorganic membranes where a sol–gel derived silica network is introduced into the polymer matrix to enhance mechanical strength, thermal stability, and proton conductivity. Indeed, non-fluorinated membranes can attain proton conductivities and power outputs approaching those of Nafion® under certain conditions, demonstrating that PFAS-free alternatives are technically feasible in principle [148]. Despite these advances, PFAS-free membranes and components still face critical durability and integration challenges. A recurring issue is insufficient chemical stability: hydrocarbon ionomers tend to degrade under the harsh oxidative and acidic conditions inside fuel cells, leading to much shorter lifetimes than PFAS-based analogues. Likewise, mechanical robustness remains a bottleneck—many non-fluorinated membranes require reinforcement to prevent excessive swelling or creep, and replacing the PTFE reinforcements or hydrophobic coatings (for example, in gas diffusion layers) has proven non-trivial. To date, most alternative materials last only on the order of tens of hours in testing, far below the >25,000 h demanded for commercial systems. Furthermore, the lack of standardized test protocols for new PFAS-free components hampers direct comparison of performance data between research groups, underscoring the need for harmonized evaluation methods going forward. In the near term, continued development should focus on extending the durability and chemical stability of these alternative materials (e.g., via improved polymer architectures, cross-linking, and fibre reinforcement) and scaling up their fabrication. Establishing common testing standards will also be critical to reliably benchmark progress across different studies and prototypes. At present, the

overall technological readiness of PFAS-free membranes and cell hardware remains low, so a concerted research effort is still required to bring these emerging materials to maturity for real-world fuel cell and electrolyser applications.

Author Contributions: Conceptualization, E.S.N. and A.B.; methodology, E.S.N. and F.B.; formal analysis, E.S.N., A.R., I.M., A.S.-V. and F.B.; investigation, E.S.N., A.R., I.M., A.S.-V. and F.B.; data curation, E.S.N., A.R., I.M., A.S.-V. and F.B.; writing—original draft preparation, E.S.N., A.R., I.M., A.S.-V. and F.B.; writing—review and editing, E.S.N., A.R., I.M., A.S.-V. and F.B.; visualization, E.S.N. and A.R.; supervision, F.B. and A.M.; project administration, F.B. and A.M.; funding acquisition, A.M.; validation, F.B. and A.M. All authors have read and agreed to the published version of the manuscript.

Funding: The activities related to the preparation of this work were supported by the FASTCH2ANGE project (GA 101192325). The project is supported by the Clean Hydrogen Partnership and its members Hydrogen Europe and Hydrogen Europe Research.

Institutional Review Board Statement: Not applicable.

Informed Consent Statement: Not applicable.

Data Availability Statement: No new data were created or analyzed in this study.

Acknowledgments: During the preparation of this work, the authors made limited use of ChatGPT (OpenAI, GPT-5.4 Thinking) for minor linguistic revision and marginal image retouching. Its use did not affect the scientific content, analysis, results, or conclusions. The authors reviewed and edited all output and took full responsibility for the final content of this publication.

Conflicts of Interest: Authors E.S.N., A.R., A.B. and A.M. were employed by the company RINA Consulting—Centro Sviluppo Materiali SpA. Author I.M. was employed by the company Il Sentiero International Campus Srl. Authors A.S.-B. and S.V. were employed by the company Tecnalia. The authors declare that the research was conducted in the absence of any commercial or financial relationships that could be construed as a potential conflict of interest.

Abbreviations

The following abbreviations are used in this manuscript:

PFAS	Per- and polyfluoroalkyl substances (materials)
PEM	Proton exchange membrane
PEMFC	Proton exchange membrane fuel cell
PEMEL	Proton exchange membrane water electrolyser (electrolysis)
IEC	Ion exchange capacity
GDL	Gas diffusion layer
LGDL	Liquid–gas diffusion layer
PTL	Porous transport layer
MEA	Membrane electrode assembly
BPP	Bipolar plates
ICR	Interfacial contact resistance
DLC	Diamond-like carbon

References

1. Brunn, H.; Arnold, G.; Körner, W.; Rippen, G.; Steinhäuser, K.G.; Valentin, I. PFAS: Forever chemicals—Persistent, bioaccumulative and mobile. Reviewing the status and the need for their phase out and remediation of contaminated sites. *Environ. Sci. Eur.* **2023**, *35*, 20. [CrossRef]
2. Sunderland, E.M.; Hu, X.C.; Dassuncao, C.; Tokranov, A.K.; Wagner, C.C.; Allen, J.G. A review of the pathways of human exposure to poly- and perfluoroalkyl substances (PFASs) and present understanding of health effects. *J. Expo. Sci. Environ. Epidemiol.* **2019**, *29*, 131–147. [CrossRef]
3. Glüge, J.; Scheringer, M.; Cousins, I.T.; DeWitt, J.C.; Goldenman, G.; Herzke, D.; Lohmann, R.; Ng, C.A.; Trier, X.; Wang, Z. An overview of the uses of per- and polyfluoroalkyl substances (PFAS). *Environ. Sci. Process. Impacts* **2020**, *22*, 2345–2373. [CrossRef]

4. Grandjean, P.; Clapp, R. Perfluorinated Alkyl Substances. *New Solut. A J. Environ. Occup. Health Policy* **2015**, *25*, 147–163. [CrossRef]
5. Renfrew, D.; Pearson, T.W. The Social Life of the "Forever Chemical". *Environ. Soc.* **2021**, *12*, 146–163. [CrossRef]
6. Kwiatkowski, C.F.; Andrews, D.Q.; Birnbaum, L.S.; Bruton, T.A.; DeWitt, J.C.; Knappe, D.R.U.; Maffini, M.V.; Miller, M.F.; Pelch, K.E.; Reade, A.; et al. Scientific Basis for Managing PFAS as a Chemical Class. *Environ. Sci. Technol. Lett.* **2020**, *7*, 532–543. [CrossRef]
7. Jha, G.; Kankarla, V.; McLennon, E.; Pal, S.; Sihi, D.; Dari, B.; Diaz, D.; Nocco, M. Per- and Polyfluoroalkyl Substances (PFAS) in Integrated Crop–Livestock Systems: Environmental Exposure and Human Health Risks. *Int. J. Environ. Res. Public Health* **2021**, *18*, 12550. [CrossRef]
8. Panieri, E.; Baralic, K.; Djukic-Cosic, D.; Buha Djordjevic, A.; Saso, L. PFAS Molecules: A Major Concern for the Human Health and the Environment. *Toxics* **2022**, *10*, 44. [CrossRef]
9. Calafat, A.M.; Wong, L.-Y.; Kuklenyik, Z.; Reidy, J.A.; Needham, L.L. Polyfluoroalkyl Chemicals in the U.S. Population: Data from the National Health and Nutrition Examination Survey (NHANES) 2003–2004 and Comparisons with NHANES 1999–2000. *Environ. Health Perspect.* **2007**, *115*, 1596–1602. [CrossRef]
10. Fenton, S.E.; Ducatman, A.; Boobis, A.; DeWitt, J.C.; Lau, C.; Ng, C.; Smith, J.S.; Roberts, S.M. Per- and Polyfluoroalkyl Substance Toxicity and Human Health Review: Current State of Knowledge and Strategies for Informing Future Research. *Environ. Toxicol. Chem.* **2020**, *40*, 606–630. [CrossRef]
11. International Agency of Research on Cancer (IARC). Perfluorooctanoic acid. In *Some Chemicals Used as Solvents and in Polymer Manufacture*; IARC-Monographs on the Evaluation of Cancerogenic Risks to Humans; International Agency of Research on Cancer: Lyon, France, 2018; Volume 110, pp. 37–110; ISBN 978-9283201762.
12. Shearer, J.J.; Callahan, C.L.; Calafat, A.M.; Huang, W.-Y.; Jones, R.R.; Sabbisetti, V.S.; Freedman, N.D.; Sampson, J.N.; Silverman, D.T.; Purdue, M.P.; et al. Serum Concentrations of Per- and Polyfluoroalkyl Substances and Risk of Renal Cell Carcinoma. *JNCI J. Natl. Cancer Inst.* **2021**, *113*, 580–587. [CrossRef]
13. Abraham, K.; Mielke, H.; Fromme, H.; Völkel, W.; Menzel, J.; Peiser, M.; Zepp, F.; Willich, S.N.; Weikert, C. Internal exposure to perfluoroalkyl substances (PFASs) and biological markers in 101 healthy 1-year-old children: Associations between levels of perfluorooctanoic acid (PFOA) and vaccine response. *Arch. Toxicol.* **2020**, *94*, 2131–2147. [CrossRef]
14. Kashino, I.; Sasaki, S.; Okada, E.; Matsuura, H.; Goudarzi, H.; Miyashita, C.; Okada, E.; Ito, Y.M.; Araki, A.; Kishi, R. Prenatal exposure to 11 perfluoroalkyl substances and fetal growth: A large-scale, prospective birth cohort study. *Environ. Int.* **2020**, *136*, 105355. [CrossRef]
15. Jin, R.; McConnell, R.; Catherine, C.; Xu, S.; Walker, D.I.; Stratakis, N.; Jones, D.P.; Miller, G.W.; Peng, C.; Conti, D.V.; et al. Perfluoroalkyl substances and severity of nonalcoholic fatty liver in Children: An untargeted metabolomics approach. *Environ. Int.* **2020**, *134*, 105220. [CrossRef]
16. Stratakis, N.; Conti, D.V.; Jin, R.; Margetaki, K.; Valvi, D.; Siskos, A.P.; Maitre, L.; Garcia, E.; Varo, N.; Zhao, Y.; et al. Prenatal Exposure to Perfluoroalkyl Substances Associated with Increased Susceptibility to Liver Injury in Children. *Hepatology* **2020**, *72*, 1758–1770. [CrossRef]
17. Lim, X. Could the world go PFAS-free? Proposal to ban 'forever chemicals' fuels debate. *Nature* **2023**, *620*, 24–27. [CrossRef]
18. European Chemicals Agency (ECHA). ECHA Publishes PFAS Restriction Proposal. Available online: https://echa.europa.eu/-/echa-publishes-pfas-restriction-proposal (accessed on 7 February 2023).
19. ECHA. Annex XV Restriction Report: Proposal for a Restriction on, Per- and Polyfluoroalkyl Substances. European Chemicals Agency, Submitted 13 January 2023 by DE, NL, DK, SE, NO. Available online: https://cdn.toxicdocs.org/Ne/NeGRqgazDBmw0wbj5VpYaR16V/NeGRqgazDBmw0wbj5VpYaR16V.pdf (accessed on 28 July 2025).
20. von Tettau, P.; Thiele, P.; Mauermann, P.; Wick, M.; Tinz, S.; Pischinger, S. Per- and polyfluoroalkyl substances in proton exchange membrane fuel cells—A review. *J. Power Sources* **2025**, *630*, 236104. [CrossRef]
21. Komers, F.; Plachá, D.; van der Bruggen, B.; Velizarov, S. Towards Sustainable Proton Exchange Membranes: Materials and Challenges for Water Electrolysis. *Water* **2025**, *17*, 3297. [CrossRef]
22. Sinha, P.; Cypher, S.M. Life Cycle Fluoropolymer Management in Proton Exchange Membrane Electrolysis. *Hydrogen* **2024**, *5*, 710–722. [CrossRef]
23. Shanmugapriya, S.; Kim, M.G.; Im, S.; Jeong, Y.; Surendran, S.; Park, T.-E.; Yun, Y.-H.; Lee, H.; Kim, T.-H.; Sim, U. Recent research trends in perfluoropolyether for energy device applications: A mini review. *J. Korean Ceram. Soc.* **2024**, *61*, 1–14. [CrossRef]
24. Hydrogen Europe. Position Paper on PFAS Restrictions: The Importance of Fluoropolymers Across the Hydrogen Value Chain, and Impacts of the Proposed PFAS Restriction for the Hydrogen Sector. Hydrogen Europe. 2023. Available online: https://hydrogeneurope.eu/wp-content/uploads/2023/02/Hydrogen-Europe-position-paper-on-PFAS-ban_v12_FINAL.pdf (accessed on 28 July 2025).

25. European Commission. Chemicals Strategy for Sustainability—Towards a Toxic-Free Environment. Brussels: European Commission. 2020. Available online: https://eur-lex.europa.eu/legal-content/EN/TXT/?uri=CELEX%3A52020DC0667 (accessed on 28 July 2025).
26. Zhao, J.; Guo, H.; Xing, Y.; Ping, S.; Lin, W.; Yang, Y.; Wang, Z.; Ma, T. A review on the sealing structure and materials of fuel-cell stacks. *Clean Energy* **2023**, *7*, 59–69. [CrossRef]
27. Olabi, A.G.; Wilberforce, T.; Alanazi, A.; Vichare, P.; Sayed, E.T.; Maghrabie, H.M.; Elsaid, K.; Abdelkareem, M.A. Novel Trends in Proton Exchange Membrane Fuel Cells. *Energies* **2022**, *15*, 4949. [CrossRef]
28. Xing, L.; Shi, W.; Su, H.; Xu, Q.; Das, P.K.; Mao, B.; Scott, K. Membrane electrode assemblies for PEM fuel cells: A review of functional graded design and optimization. *Energy* **2019**, *177*, 445–464. [CrossRef]
29. Yang, G.; Lee, C.; Qiao, X.; Babu, S.K.; Martinez, U.; Spendelow, J.S. Advanced Electrode Structures for Proton Exchange Membrane Fuel Cells: Current Status and Path Forward. *Electrochem. Energy Rev.* **2024**, *7*, 9. [CrossRef]
30. Sezer, N.; Bayhan, S.; Fesli, U.; Sanfilippo, A. A comprehensive review of the state-of-the-art of proton exchange membrane water electrolysis. *Mater. Sci. Energy Technol.* **2025**, *8*, 44–65. [CrossRef]
31. Sayed-Ahmed, H.; Toldy, Á.I.; Santasalo-Aarnio, A. Dynamic operation of proton exchange membrane electrolyzers—Critical review. *Renew. Sustain. Energy Rev.* **2024**, *189*, 113883. [CrossRef]
32. Shiva Kumar, S.; Himabindu, V. Hydrogen production by PEM water electrolysis—A review. *Mater. Sci. Energy Technol.* **2019**, *2*, 442–454. [CrossRef]
33. Swedish Chemicals Agency (KEMI). *What You Need to Know About the Updated PFAS Restriction Dossier*; KEMI: Stockholm, Sweden, 2025.
34. Wang, C.R.; Stansberry, J.M.; Mukundan, R.; Chang, H.-M.J.; Kulkarni, D.; Park, A.M.; Plymill, A.B.; Firas, N.M.; Liu, C.P.; Lang, J.T.; et al. Proton Exchange Membrane (PEM) Water Electrolysis: Cell-Level Considerations for Gigawatt-Scale Deployment. *Chem. Rev.* **2025**, *125*, 1257–1302. [CrossRef]
35. Wang, T.; Cao, X.; Jiao, L. PEM water electrolysis for hydrogen production: Fundamentals, advances, and prospects. *Carbon Neutrality* **2022**, *1*, 21. [CrossRef]
36. Moshtarikhah, S.; Oppers, N.A.W.; de Groot, M.T.; Keurentjes, J.T.F.; Schouten, J.C.; van der Schaaf, J. Nernst–Planck modeling of multicomponent ion transport in a Nafion membrane at high current density. *J. Appl. Electrochem.* **2017**, *47*, 51–62. [CrossRef]
37. Ludlam, G.A.H.; Gnaniah, S.J.P.; Degl'Innocenti, R.; Gupta, G.; Wain, A.J.; Lin, H. Measurement of Water Uptake and States in Nafion Membranes Using Humidity-Controlled Terahertz Time-Domain Spectroscopy. *ACS Sustain. Chem. Eng.* **2024**, *12*, 7924–7934. [CrossRef]
38. Sun, X.; Simonsen, S.; Norby, T.; Chatzitakis, A. Composite Membranes for High Temperature PEM Fuel Cells and Electrolysers: A Critical Review. *Membranes* **2019**, *9*, 83. [CrossRef]
39. Kerres, J.A. Development of ionomer membranes for fuel cells. *J. Membr. Sci.* **2001**, *185*, 3–27. [CrossRef]
40. Wilberforce, T.; Khatib, F.N.; Ijaodola, O.S.; Ogungbemi, E.; El-Hassan, Z.; Durrant, A.; Thompson, J.; Olabi, A.G. Numerical modelling and CFD simulation of a polymer electrolyte membrane (PEM) fuel cell flow channel using an open pore cellular foam material. *Sci. Total Environ.* **2019**, *678*, 728–740. [CrossRef]
41. Teng, H. Overview of the Development of the Fluoropolymer Industry. *Appl. Sci.* **2012**, *2*, 496–512. [CrossRef]
42. Kreuer, K.D. On the development of proton conducting polymer membranes for hydrogen and methanol fuel cells. *J. Membr. Sci.* **2001**, *185*, 29–39. [CrossRef]
43. Zanchet, L.; da Trindade, L.G.; Trombetta, F.; Martins, A.D.; Martini, E.M.; Becker, M.R.; de Souza, M.O. Improving Nafion/zeolite nanocomposite with a $CF_3SO_3^-$ based ionic liquid for PEMFC application. *Ionics* **2021**, *27*, 2027–2036. [CrossRef]
44. Millet, P.; Ngameni, R.; Grigoriev, S.A.; Mbemba, N.; Brisset, F.; Ranjbari, A.; Etiévant, C. PEM water electrolyzers: From electrocatalysis to stack development. *Int. J. Hydrogen Energy* **2010**, *35*, 5043–5052. [CrossRef]
45. Huo, Y.; Li, Q.; Rui, Z.; Ding, R.; Liu, J.; Li, J.; Liu, J. A highly stable reinforced PEM assisted by resveratrol and polydopamine-treated PTFE. *J. Membr. Sci.* **2021**, *635*, 119453. [CrossRef]
46. Chen, T.; Lv, B.; Sun, S.; Hao, J.; Shao, Z. Novel Nafion/Graphitic Carbon Nitride Nanosheets Composite Membrane for Steam Electrolysis at 110 °C. *Membranes* **2023**, *13*, 308. [CrossRef]
47. Park, C.W.; Jeong, E.; Kim, I.; Kim, H.-J.; Yang, H.-M.; Sihn, Y.-H.; Yoon, I.-H. Combined water electrolysis and 2D hydron separator for enhanced hydrogen isotope separation. *Chem. Eng. J.* **2024**, *498*, 155328. [CrossRef]
48. Ruhkopf, J.; Plachetka, U.; Moeller, M.; Pasdag, O.; Radev, I.; Peinecke, V.; Hepp, M.; Wiktor, C.; Lohe, M.R.; Feng, X.; et al. Graphene Coating of Nafion Membranes for Enhanced Fuel Cell Performance. *ACS Appl. Eng. Mater.* **2023**, *1*, 947–954. [CrossRef] [PubMed]
49. Kwon, O.; Oh, K.; Park, J.; Park, S.; Lee, T.G.; Son, B. Morphological structure of silica sulfuric acid and Nafion composite membrane using electrostatic force microscopy. *Int. J. Energy Res.* **2021**, *45*, 21195–21208. [CrossRef]
50. Teixeira, F.C.; Teixeira, A.P.S.; Rangel, C.M. New Modified SPEEK-Based Proton Exchange Membranes. *Polymers* **2025**, *17*, 1646. [CrossRef]

51. Liu, X.; Zhang, Y.; Chen, Y.; Li, C.; Dong, J.; Zhang, Q.; Wang, J.; Yang, Z.; Cheng, H. A superhydrophobic bromomethylated poly(phenylene oxide) as a multifunctional polymer filler in SPEEK membrane towards neat methanol operation of direct methanol fuel cells. *J. Membr. Sci.* **2017**, *544*, 58–67. [CrossRef]
52. Li, W.; Jiang, J.; An, H.; Dong, S.; Yue, Z.; Qian, H.; Yang, H. Self-Cross-Linked Sulfonated Poly(ether ether ketone) with Pendant Sulfoalkoxy Groups for Proton Exchange Membrane Fuel Cells. *ACS Appl. Energy Mater.* **2021**, *4*, 2732–2740. [CrossRef]
53. Wang, S.; Zhu, T.; Shi, B.; Fan, C.; Liu, Y.; Yin, Z.; Gao, Z.; Zhang, Z.; Wu, H.; Jiang, Z. Porous organic polymer with high-density phosphoric acid groups as filler for hybrid proton exchange membranes. *J. Membr. Sci.* **2023**, *666*, 121147. [CrossRef]
54. Wu, J.; Wang, F.; Fan, X.; Chu, J.; Cheng, F.; Hu, F.; Liu, H.; Zhang, Q.; Xu, Z.; Gong, C. Phosphoric acid-doped Gemini quaternary ammonium-grafted SPEEK membranes with superhigh proton conductivity and mechanical strength for direct methanol fuel cells. *J. Membr. Sci.* **2023**, *672*, 121431. [CrossRef]
55. Chu, J.; Ou, Y.; Cheng, F.; Liu, H.; Luo, N.; Hu, F.; Wen, S.; Gong, C. Achieving better balance on the mechanical stability and conduction performance of sulfonated poly(ether ether ketone) proton exchange membranes through polydopamine/polyethyleneimine co-modified poly(vinylidene fluoride) nanofiber as support. *Int. J. Hydrogen Energy* **2024**, *50*, 1381–1390. [CrossRef]
56. Sharma, V.; Upadhyay, P.; Rathod, N.H.; Sharma, J.; Mishra, S.; Raj, S.K.; Kishore, V.; Kulshrestha, V. Silica modified sulphonated Poly(ether ether ketone) proton exchange membranes for DMFC application. *Int. J. Hydrogen Energy* **2023**, *48*, 37784–37795. [CrossRef]
57. Kim, A.R.; Vinothkannan, M.; Lee, K.H.; Chu, J.Y.; Park, B.; Han, M.; Yoo, D.J. Enhanced performance and durability of composite membranes containing anatase titanium oxide for fuel cells operating under low relative humidity. *Int. J. Energy Res.* **2022**, *46*, 4835–4851. [CrossRef]
58. Ahmad, S.; Nawaz, T.; Ali, A.; Orhan, M.F.; Samreen, A.; Kannan, A.M. An overview of proton exchange membranes for fuel cells: Materials and manufacturing. *Int. J. Hydrogen Energy* **2022**, *47*, 19086–19131. [CrossRef]
59. Iulianelli, A.; Basile, A. Sulfonated PEEK-based polymers in PEMFC and DMFC applications: A review. *Int. J. Hydrogen Energy* **2012**, *37*, 15241–15255. [CrossRef]
60. Mahato, N.; Jang, H.; Dhyani, A.; Cho, S. Recent Progress in Conducting Polymers for Hydrogen Storage and Fuel Cell Applications. *Polymers* **2020**, *12*, 2480. [CrossRef]
61. Adamski, M.; Peressin, N.; Holdcroft, S. On the evolution of sulfonated polyphenylenes as proton exchange membranes for fuel cells. *Mater. Adv.* **2021**, *2*, 4966–5005. [CrossRef]
62. Palamara, D.; Bruzzaniti, P.; Calabrese, L.; Proverbio, E. Effect of degree of sulfonation on the performance of adsorbent SAPO-34/S-PEEK composite coatings for adsorption heat pumps. *Prog. Org. Coat.* **2021**, *154*, 106193. [CrossRef]
63. Egemole, F.O.; Biancolli, A.L.G.; Holdcroft, S. Water electrolysis using fluorine-free, reinforced sulfo-phenylated polyphenylene membranes. *Electrochim. Acta* **2024**, *508*, 145259. [CrossRef]
64. KoE, J.; Lee, E.; Lee, J.Y.; Yu, D.M.; Yoon, S.J.; Oh, K.-H.; Hong, Y.T.; So, S. Multi-Block Copolymer Membranes Consisting of Sulfonated Poly(p-phenylene) and Naphthalene Containing Poly(arylene Ether Ketone) for Proton Exchange Membrane Water Electrolysis. *Polymers* **2023**, *15*, 1748. [CrossRef]
65. Duan, Y.; Ru, C.; Li, J.; Sun, Y.; Pu, X.; Liu, B.; Pang, B.; Zhao, C. Enhancing proton conductivity and methanol resistance of SPAEK membrane by incorporating MOF with flexible alkyl sulfonic acid for DMFC. *J. Membr. Sci.* **2022**, *641*, 119906. [CrossRef]
66. Liu, Y.; Huo, P.; Ren, J.; Wang, G. Organic–inorganic hybrid proton-conducting electrolyte membranes based on sulfonated poly(arylene ether sulfone) and SiO_2–SO_3H network for fuel cells. *High Perform. Polym.* **2017**, *29*, 1037–1048. [CrossRef]
67. Liu, Z.; Wang, P.; Hu, W.; Liu, B. Preparation and Properties of Hybrid Silane-crosslinked Sulfonated Poly(aryl ether ketone)s as Proton Exchange Membranes. *Chem. Res. Chin. Univ.* **2019**, *35*, 937–944. [CrossRef]
68. Perrot, C.; Gonon, L.; Marestin, C.; Gebel, G. Hydrolytic degradation of sulfonated polyimide membranes for fuel cells. *J. Membr. Sci.* **2011**, *379*, 207–214. [CrossRef]
69. Afzal, J.; Wang, H. A review on sulfonated organic polymer based composite membranes for PEM water electrolyzers. *Int. J. Hydrogen Energy* **2025**, *123*, 100–117. [CrossRef]
70. Kausar, A. Progression from Polyimide to Polyimide Composite in Proton-Exchange Membrane Fuel Cell: A Review. *Polym.-Plast. Technol. Eng.* **2017**, *56*, 1375–1390. [CrossRef]
71. Hooshyari, K.; Rezania, H.; Vatanpour, V.; Salarizadeh, P.; Askari, M.B.; Beydaghi, H.; Enhessari, M. High temperature membranes based on PBI/sulfonated polyimide and doped-perovskite nanoparticles for PEM fuel cells. *J. Membr. Sci.* **2020**, *612*, 118436. [CrossRef]
72. You, P.Y.; Kamarudin, S.K.; Masdar, M.S. Improved performance of sulfonated polyimide composite membranes with rice husk ash as a bio-filler for application in direct methanol fuel cells. *Int. J. Hydrogen Energy* **2019**, *44*, 1857–1866. [CrossRef]
73. Hu, M.; Zhang, B.; Chen, J.; Xu, M.; Liu, D.; Wang, L. Cross-linked polymer electrolyte membrane based on a highly branched sulfonated polyimide with improved electrochemical properties for fuel cell applications. *Int. J. Energy Res.* **2019**, *43*, 8753–8764. [CrossRef]

74. Rehman, W.; Liaqat, K.; Fazil, S.; Saeed, S.; Waseem, M.; Shakeel, M.; Mir, S.; Bibi, I.; Guo, C.-Y. Chemically tethered functionalized graphene oxide based novel sulfonated polyimide composite for polymer electrolyte membrane. *J. Polym. Res.* **2019**, *26*, 82. [CrossRef]
75. Jiang, G.; Zhang, J.; Qiao, J.; Jiang, Y.; Zarrin, H.; Chen, Z.; Hong, F. Bacterial nanocellulose/Nafion composite membranes for low temperature polymer electrolyte fuel cells. *J. Power Sources* **2015**, *273*, 697–706. [CrossRef]
76. Mohanapriya, S.; Rambabu, G.; Bhat, S.D.; Raj, V. Pectin based nanocomposite membranes as green electrolytes for direct methanol fuel cells. *Arab. J. Chem.* **2020**, *13*, 2024–2040. [CrossRef]
77. Nasirinezhad, M.; Ghaffarian, S.R.; Tohidian, M. Nanocomposite Membranes Based on Imidazole-Functionalized Chitin Nanowhiskers for Direct Methanol Fuel Cell Applications. *J. Macromol. Sci. Part B* **2021**, *60*, 663–685. [CrossRef]
78. Munavalli, B.; Torvi, A.; Kariduraganavar, M. A facile route for the preparation of proton exchange membranes using sulfonated side chain graphite oxides and crosslinked sodium alginate for fuel cell. *Polymer* **2018**, *142*, 293–309. [CrossRef]
79. Rosli, N.A.H.; Loh, K.S.; Wong, W.Y.; Yunus, R.M.; Lee, T.K.; Ahmad, A.; Chong, S.T. Review of Chitosan-Based Polymers as Proton Exchange Membranes and Roles of Chitosan-Supported Ionic Liquids. *Int. J. Mol. Sci.* **2020**, *21*, 632. [CrossRef]
80. Melo, S.; Deus, E.; Montezuma, M.; Ruchert, C.; Carvalho, M. Chitosan Composites Modified with Nano-Cellulose and Graphene Oxide for Proton Exchange Membrane (Pem) Electrolyzers. *SSRN* **2025**. [CrossRef]
81. Divya, K.; Rana, D.; Alwarappan, S.; Abirami Saraswathi, M.S.S.; Nagendran, A. Investigating the usefulness of chitosan based proton exchange membranes tailored with exfoliated molybdenum disulfide nanosheets for clean energy applications. *Carbohydr. Polym.* **2019**, *208*, 504–512. [CrossRef]
82. Liu, H.; Gong, C.; Wang, J.; Liu, X.; Liu, H.; Cheng, F.; Wang, G.; Zheng, G.; Qin, C.; Wen, S. Chitosan/silica coated carbon nanotubes composite proton exchange membranes for fuel cell applications. *Carbohydr. Polym.* **2016**, *136*, 1379–1385. [CrossRef]
83. Araya, S.S.; Zhou, F.; Liso, V.; Sahlin, S.L.; Vang, J.R.; Thomas, S.; Gao, X.; Jeppesen, C.; Kær, S.K. A comprehensive review of PBI-based high temperature PEM fuel cells. *Int. J. Hydrogen Energy* **2016**, *41*, 21310–21344. [CrossRef]
84. Aili, D.; Hansen, M.K.; Pan, C.; Li, Q.; Christensen, E.; Jensen, J.O.; Bjerrum, N.J. Phosphoric acid doped membranes based on Nafion®, PBI and their blends—Membrane preparation, characterization and steam electrolysis testing. *Int. J. Hydrogen Energy* **2011**, *36*, 6985–6993. [CrossRef]
85. Garbe, S.; Futter, J.; Schmidt, T.J.; Gubler, L. Insight into elevated temperature and thin membrane application for high efficiency in polymer electrolyte water electrolysis. *Electrochim. Acta* **2021**, *377*, 138046. [CrossRef]
86. Maiti, T.K.; Singh, J.; Majhi, J.; Ahuja, A.; Maiti, S.; Dixit, P.; Bhushan, S.; Bandyopadhyay, A.; Chattopadhyay, S. Advances in polybenzimidazole based membranes for fuel cell applications that overcome Nafion membranes constraints. *Polymer* **2022**, *255*, 125151. [CrossRef]
87. Plackett, D.; Siu, A.; Li, Q.; Pan, C.; Jensen, J.O.; Nielsen, S.F.; Permyakova, A.A.; Bjerrum, N.J. High-temperature proton exchange membranes based on polybenzimidazole and clay composites for fuel cells. *J. Membr. Sci.* **2011**, *383*, 78–87. [CrossRef]
88. Ghosh, P.; Mandal, S.; Majumdar, S.; Sarkar, A.; Ganguly, S.; Kargupta, K. Enhanced power generation, faster transient response and longer durability of HT-PEMFC using composite polybenzimidazole electrolyte membrane with optimum rGO loading. *Int. J. Hydrogen Energy* **2020**, *45*, 16708–16723. [CrossRef]
89. Sakthivel, V.; Bhagyalakshmi, P.; Kim, A.R.; Sayfiddinov, D.; Vijayapradeep, S.; Yoo, D.J. Synergistic Acid–Base Interfaces in Phosphoric Acid-Doped Polymer Electrolytes for Efficient H_2/O_2Fuel Cells. *ACS Appl. Mater. Interfaces* **2025**, *17*, 58740–58752. [CrossRef] [PubMed]
90. Doan, T.L.; Lee, H.E.; Shah, S.S.H.; Kim, M.; Kim, C.; Cho, H.; Kim, T. A review of the porous transport layer in polymer electrolyte membrane water electrolysis. *Int. J. Energy Res.* **2021**, *45*, 14207–14220. [CrossRef]
91. Arbabi, F.; Kalantarian, A.; Abouatallah, R.; Wang, R.; Wallace, J.S.; Bazylak, A. Feasibility study of using microfluidic platforms for visualizing bubble flows in electrolyzer gas diffusion layers. *J. Power Sources* **2014**, *258*, 142–149. [CrossRef]
92. Tirumalasetti, P.R.; Weng, F.-B.; Dlamini, M.M.; Atabani, A.; Jung, G.-B.; Yu, J.-W.; Abbas, W.; Hsu, C.-Y. A review on performance and two-phase flow in proton exchange membrane water electrolyzers using porous transport layers and high-speed visualization. *Int. J. Hydrogen Energy* **2025**, *144*, 513–521. [CrossRef]
93. Amores, E.; Sánchez, M.; Rojas, N.; Sánchez-Molina, M. Renewable hydrogen production by water electrolysis. In *Sustainable Fuel Technologies Handbook*; Elsevier: Amsterdam, The Netherlands, 2021; pp. 271–313. [CrossRef]
94. Lee, F.C.; Ismail, M.S.; Ingham, D.B.; Hughes, K.J.; Ma, L.; Lyth, S.M.; Pourkashanian, M. Alternative architectures and materials for PEMFC gas diffusion layers: A review and outlook. *Renew. Sustain. Energy Rev.* **2022**, *166*, 112640. [CrossRef]
95. Yoon, G.H.; Park, S.B.; Kim, E.H.; Oh, M.H.; Cho, K.S.; Jeong, S.W.; Kim, S.; Park, Y. Il Novel Hydrophobic Coating Process for Gas Diffusion Layer in PEMFCs. *J. Electroceramics* **2009**, *23*, 110–115. [CrossRef]
96. Sun, Y.; Liu, W.; Xu, D.; Li, X.; Li, C. Self-Healing of Super Hydrophobic and Hierarchical Surfaces for Gas Diffusion Layer. *Int. J. Hydrogen Energy* **2020**, *45*, 29774–29781. [CrossRef]

97. Öztürk, A.; BayrakçekenYurtcan, A. Investigation of Synergetic Effect of PDMS Polymer Hydrophobicity and Polystyrene-Silica Particles Roughness in the Content of Microporous Layer on Water Management in PEM Fuel Cell. *Appl. Surf. Sci.* **2020**, *511*, 145415. [CrossRef]
98. Wang, Y.; Saher, S.; Li, X. Fabrication of Hydrophobic Coating on GDL with Silicone Based Materials. *ECS Meet. Abstr.* **2010**, *MA2010-01*, 559. [CrossRef]
99. Iyer, R.; Kelly, J.; Elgowainy, A. *Electrolyzers for Hydrogen Production: Solid Oxide, Alkaline, and Proton Exchange Membrane*; Argonne National Laboratory: Argonne, IL, USA, 2022. [CrossRef]
100. Feng, J.; Zhang, Q.; Tu, Z.; Tu, W.; Wan, Z.; Pan, M.; Zhang, H. Degradation of silicone rubbers with different hardness in various aqueous solutions. *Polym. Degrad. Stab.* **2014**, *109*, 122–128. [CrossRef]
101. Kömmling, A.; Jaunich, M.; Pourmand, P.; Wolff, D.; Hedenqvist, M. Analysis of O-Ring Seal Failure under Static Conditions and Determination of End-of-Lifetime Criterion. *Polymers* **2019**, *11*, 1251. [CrossRef] [PubMed]
102. Cui, T.; Chao, Y.J.; Chen, X.M.; van Zee, J.W. Effect of water on life prediction of liquid silicone rubber seals in polymer electrolyte membrane fuel cell. *J. Power Sources* **2011**, *196*, 9536–9543. [CrossRef]
103. Basuli, U.; Jose, J.; Lee, R.H.; Yoo, Y.H.; Jeong, K.-U.; Ahn, J.-H.; Nah, C. Properties and Degradation of the Gasket Component of a Proton Exchange Membrane Fuel Cell—A Review. *J. Nanosci. Nanotechnol.* **2012**, *12*, 7641–7657. [CrossRef]
104. Patel, H. Experimental and Advanced Computational Modelling Study of Downhole Elastomer Seal Assemblies. Ph.D. Thesis, University of Oklahoma, Norman, OK, USA, 2020. Available online: https://hdl.handle.net/11244/324324 (accessed on 28 July 2025).
105. Yoo, J.; Lee, Y.H.; Park, J.; Oh, H.-S.; An, J.-H.; Joo, W.-J.; Kim, M.S. Study on low temperature and durability characteristics of gasket for polymer electrolyte membrane fuel cell (PEMFC) depending on cross-sectional geometry. *Int. J. Hydrogen Energy* **2024**, *50*, 1194–1206. [CrossRef]
106. Pehlivan-Davis, S. Polymer Electrolyte Membrane (PEM) Fuel Cell Seals Durability. Ph.D. Thesis, Loughborough University, Leicestershire, UK, 2016. Available online: https://hdl.handle.net/2134/21749 (accessed on 28 July 2025).
107. Wood, D.L.; Borup, R.L. Durability Aspects of Gas-Diffusion and Microporous Layers. In *Polymer Electrolyte Fuel Cell Durability*; Springer: New York, NY, USA, 2009; pp. 159–195. [CrossRef]
108. Mitra, S.; Ghanbari-Siahkali, A.; Kingshott, P.; Almdal, K.; Kem Rehmeier, H.; Christensen, A.G. Chemical degradation of fluoroelastomer in an alkaline environment. *Polym. Degrad. Stab.* **2004**, *83*, 195–206. [CrossRef]
109. Tan, J.; Chao, Y.J.; van Zee, J.W.; Lee, W.K. Degradation of elastomeric gasket materials in PEM fuel cells. *Mater. Sci. Eng. A* **2007**, *445–446*, 669–675. [CrossRef]
110. Lin, C.-W.; Chien, C.-H.; Tan, J.; Chao, Y.J.; van Zee, J.W. Chemical degradation of five elastomeric seal materials in a simulated and an accelerated PEM fuel cell environment. *J. Power Sources* **2011**, *196*, 1955–1966. [CrossRef]
111. Qiu, D.; Liang, P.; Peng, L.; Yi, P.; Lai, X.; Ni, J. Material behavior of rubber sealing for proton exchange membrane fuel cells. *Int. J. Hydrogen Energy* **2020**, *45*, 5465–5473. [CrossRef]
112. Derham, C. Transient effects influencing sealing force in elasomeric O ring seals. *Plast. Rubber Compos. Process. Appl.* **1997**, *26*, 129–136.
113. Prasad, K.; Nikzad, M.; Sbarski, I. Permeability control in polymeric systems: A review. *J. Polym. Res.* **2018**, *25*, 232. [CrossRef]
114. Foltuț, D.; Șerban, V.-A. Current Advancements in the Behavior Analysis of EPDM Elastomers in Peripheral Applications of the Cathodic Side of PEMFC Systems. *Recent Prog. Mater.* **2024**, *6*, 1–27. [CrossRef]
115. Momenifar, M.; Ghadimi, M.; Barzegari, M.; Mohammadi, K. Mechanical and chemical characteristics of the PEM fuel cell sealants in simulated environment. *Hydrog. Fuel Cell Energy Storage* **2022**, *9*, 163–178. [CrossRef]
116. Shamsabadi, A.; Farahani, A.; Shirkavand, M.M.; Hafezi, M.-J.; Tohidian, M. Carbon black/ethylene propylene diene monomer (EPDM) rubber as polymer electrolyte membrane fuel cell gaskets: Mechanical and chemical assessment. *Iran. Polym. J.* **2024**, *33*, 169–183. [CrossRef]
117. Kang, H.M.; Choi, M.C.; Lee, J.H.; Yun, Y.M.; Jang, J.S.; Chung, N.K.; Jeon, S.K.; Jung, J.K.; Lee, J.H.; Lee, J.H.; et al. Effect of the High-Pressure Hydrogen Gas Exposure in the Silica-Filled EPDM Sealing Composites with Different Silica Content. *Polymers* **2022**, *14*, 1151. [CrossRef]
118. Wu, F.; Chen, B.; Pan, M. Degradation of the Sealing Silicone Rubbers in a Proton Exchange Membrane Fuel Cell at Cold Start Conditions. *Int. J. Electrochem. Sci.* **2020**, *15*, 3013–3028. [CrossRef]
119. Yan, F.; Zhang, X.; Liu, F.; Li, X.; Zhang, Z. Adjusting the properties of silicone rubber filled with nanosilica by changing the surface organic groups of nanosilica. *Compos. Part B Eng.* **2015**, *75*, 47–52. [CrossRef]
120. Liu, D.; Song, L.; Song, H.; Chen, J.; Tian, Q.; Chen, L.; Sun, L.; Lu, A.; Huang, C.; Sun, G. Correlation between mechanical properties and microscopic structures of an optimized silica fraction in silicone rubber. *Compos. Sci. Technol.* **2018**, *165*, 373–379. [CrossRef]
121. Sim, Y.L.; Lee, J.; Oh, S.M.; Kim, D.B.; Kim, K.; Baeck, S.-H.; Shim, S.E.; Qian, Y. Mitigation of Silicon Contamination in Fuel Cell Gasket Materials through Silica Surface Treatment. *Polymers* **2024**, *16*, 914. [CrossRef] [PubMed]

122. Frisch, L. PEM fuel cell stack sealing using silicone elastomers. *Seal. Technol.* **2001**, *2001*, 7–9. [CrossRef]
123. Irshad, H.M.; Shahgaldi, S. Comprehensive review of bipolar plates for proton exchange membrane fuel cells with a focus on materials, processing methods and characteristics. *Int. J. Hydrogen Energy* **2025**, *111*, 462–487. [CrossRef]
124. Tawfik, H.; Hung, Y.; Mahajan, D. Metal bipolar plates for PEM fuel cell—A review. *J. Power Sources* **2007**, *163*, 755–767. [CrossRef]
125. Ijaodola, O.; Ogungbemi, E.; Khatib, F.N.; Wilberforce, T.; Ramadan, M.; el Hassan, Z.; Thompson, J.; Olabi, A.G. Evaluating the Effect of Metal Bipolar Plate Coating on the Performance of Proton Exchange Membrane Fuel Cells. *Energies* **2018**, *11*, 3203. [CrossRef]
126. Xu, J.; Xu, S.; Munroe, P.; Xie, Z.-H. A ZrN nanocrystalline coating for polymer electrolyte membrane fuel cell metallic bipolar plates prepared by reactive sputter deposition. *RSC Adv.* **2015**, *5*, 67348–67356. [CrossRef]
127. Mi, B.; Wang, Q.; Xu, Y.; Qin, Z.; Chen, Z.; Wang, H. Improvement in Corrosion Resistance and Interfacial Contact Resistance Properties of 316L Stainless Steel by Coating with Cr, Ti Co-Doped Amorphous Carbon Films in the Environment of the PEMFCs. *Molecules* **2023**, *28*, 2821. [CrossRef] [PubMed]
128. Mi, B.; Chen, T.; Zhang, J.; Ma, X.; Wang, J.; Liu, P.; Wang, H.; Li, W. Effect of N doping on Cr-doped amorphous carbon/CrN/Ti multilayer coatings on 316L stainless steel bipolar plate for PEMFC: First principles calculation, structure and performance. *Int. J. Hydrogen Energy* **2024**, *71*, 1303–1316. [CrossRef]
129. Huang, Y. Corrosion Resistance, Interfacial Contact Resistance, and Hydrophobicity of 316L Stainless Steel Bipolar Plates Coated with TiN/Amorphous Carbon Double Layer under Different Carbon Target Currents. *Coatings* **2023**, *13*, 1494. [CrossRef]
130. Heo, H.-S.; Kim, S.-J. Investigation of Electrochemical Characteristics and Interfacial Contact Resistance of TiN-Coated Titanium as Bipolar Plate in Polymer Electrolyte Membrane Fuel Cell. *Coatings* **2023**, *13*, 123. [CrossRef]
131. Li, T.; Yan, Z.; Liu, Z.; Yan, Y.; Chen, Y. Surface microstructure and performance of TiN monolayer film on titanium bipolar plate for PEMFC. *Int. J. Hydrogen Energy* **2021**, *46*, 31382–31390. [CrossRef]
132. Turan, C.; Cora, Ö.N.; Koç, M. Investigation of the effects of process sequence on the contact resistance characteristics of coated metallic bipolar plates for polymer electrolyte membrane fuel cells. *J. Power Sources* **2013**, *243*, 925–934. [CrossRef]
133. Hedayati, A.; Asghari, S.; Alinoori, A.H.; Koosha, M.; Vuorinen, E. Effects of coating thickness on corrosion and contact resistance behavior of TiN coated AISI 316L as bipolar plates for PEMFC. *Hydrog. Fuel Cell Energy Storage* **2017**, *3*, 137–149. [CrossRef]
134. Wang, L.; Tao, Y.; Zhang, Z.; Wang, Y.; Feng, Q.; Wang, H.; Li, H. Molybdenum carbide coated 316L stainless steel for bipolar plates of proton exchange membrane fuel cells. *Int. J. Hydrogen Energy* **2019**, *44*, 4940–4950. [CrossRef]
135. He, R.Y.; Jiang, J.; Wang, R.F.; Yue, Y.; Chen, Y.; Pan, T.J. Anti-corrosion and conductivity of titanium diboride coating on metallic bipolar plates. *Corros. Sci.* **2020**, *170*, 108646. [CrossRef]
136. Lu, J.L.; Abbas, N.; Tang, J.; Hu, R.; Zhu, G.M. Characterization of Ti_3SiC_2-coating on stainless steel bipolar plates in simulated proton exchange membrane fuel cell environments. *Electrochem. Commun.* **2019**, *105*, 106490. [CrossRef]
137. Ma, G.; Zhang, D.; Guo, P.; Li, H.; Xin, Y.; Wang, Z.; Wang, A. Phase orientation improved the corrosion resistance and conductivity of Cr2AlC coatings for metal bipolar plates. *J. Mater. Sci. Technol.* **2022**, *105*, 36–44. [CrossRef]
138. Nguyen, H.; Lombeck, F.; Schwarz, C.; Heizmann, P.A.; Adamski, M.; Lee, H.-F.; Britton, B.; Holdcroft, S.; Vierrath, S.; Breitwieser, M. Hydrocarbon-based Pemion^{TM} proton exchange membrane fuel cells with state-of-the-art performance. *Sustain. Energy Fuels* **2021**, *5*, 3687–3699. [CrossRef]
139. European Union. Development of Non-Fluorinated Components for Fuel Cells and Electrolysers. CORDIS. Available online: https://cordis.europa.eu/programme/id/HORIZON_HORIZON-JTI-CLEANH2-2024-05-02/en (accessed on 18 December 2023).
140. Nguyen, H.; Klose, C.; Metzler, L.; Vierrath, S.; Breitwieser, M. Fully Hydrocarbon Membrane Electrode Assemblies for Proton Exchange Membrane Fuel Cells and Electrolyzers: An Engineering Perspective. *Adv. Energy Mater.* **2022**, *12*, 2103559. [CrossRef]
141. Lim, X. What it will take to reach a PFAS-free future. *Chem. Eng. News* **2025**, 103. Available online: https://cen.acs.org/materials/take-PFAS-free-future/103/web/2025/04 (accessed on 28 July 2025).
142. Kraytsberg, A.; Ein-Eli, Y. Review of Advanced Materials for Proton Exchange Membrane Fuel Cells. *Energy Fuels* **2014**, *28*, 7303–7330. [CrossRef]
143. Han, S.-Y.; Yu, D.M.; Mo, Y.-H.; Ahn, S.M.; Lee, J.Y.; Kim, T.-H.; Yoon, S.J.; Hong, S.; Hong, Y.T.; So, S. Ion exchange capacity controlled biphenol-based sulfonated poly(arylene ether sulfone) for polymer electrolyte membrane water electrolyzers: Comparison of random and multi-block copolymers. *J. Membr. Sci.* **2021**, *634*, 119370. [CrossRef]
144. Krasae-in, S. Optimal operation of a large-scale liquid hydrogen plant utilizing mixed fluid refrigeration system. *Int. J. Hydrogen Energy* **2014**, *39*, 7015–7029. [CrossRef]
145. di Virgilio, M.; Basso Peressut, A.; Arosio, V.; Arrigoni, A.; Latorrata, S.; Dotelli, G. Functional and Environmental Performances of Novel Electrolytic Membranes for PEM Fuel Cells: A Lab-Scale Case Study. *Clean Technol.* **2023**, *5*, 74–93. [CrossRef]
146. Balogun, E. Non-Fluorous Hydrocarbon Ionomers as Substitutes for Perfluorosulfonic Acid Ionomers in Polymer Electrolyte Membrane Fuel Cell Applications. Ph.D. Thesis, Simon Fraser University, Burnaby, BC, Canada, 2023. Available online: https://summit.sfu.ca/item/38019 (accessed on 28 July 2025).

147. European Environment Agency. PFAS Polymers in Focus. 2024. Available online: https://www.eea.europa.eu/en/analysis/publications/pfas-polymers-in-focus (accessed on 28 July 2025).
148. Hydrogen Europe. Position Paper on PFAS Ban and its Impact on the Hydrogen Sector. 2022. Available online: https://www.esaknowledgebase.com/wp-content/uploads/2022/04/Hydrogen-Europe-position-paper-on-PFAS-ban_v6.pdf (accessed on 28 July 2025).

Disclaimer/Publisher's Note: The statements, opinions and data contained in all publications are solely those of the individual author(s) and contributor(s) and not of MDPI and/or the editor(s). MDPI and/or the editor(s) disclaim responsibility for any injury to people or property resulting from any ideas, methods, instructions or products referred to in the content.